

Review

# Recent Insights in Transition Metal Sulfide Hydrodesulfurization Catalysts for the Production of Ultra Low Sulfur Diesel: A Short Review

Jorge Noé Díaz de León \*, Chowdari Ramesh Kumar, Joel Antúnez-García and Sergio Fuentes-Moyado

Centro de Nanociencias y Nanotecnología, Universidad Nacional Autónoma de México, Km. 107 Carretera Tijuana-Ensenada Col. Pedregal Playitas, C. P. 22860 Ensenada, Baja California, Mexico; chowdarirameshkumar@gmail.com (C.R.K.); joel.antunez@gmail.com (J.A.-G.); fuentes@cnyun.unam.mx (S.F.-M.)

\* Correspondence: noejd@cnyun.unam.mx

Received: 29 November 2018; Accepted: 7 January 2019; Published: 15 January 2019



**Abstract:** The literature from the past few years dealing with hydrodesulfurization catalysts to deeply remove the sulfur-containing compounds in fuels is reviewed in this communication. We focus on the typical transition metal sulfides (TMS) Ni/Co-promoted Mo, W-based bi- and tri-metallic catalysts for selective removal of sulfur from typical refractory compounds. This review is separated into three very specific topics of the catalysts to produce ultra-low sulfur diesel. The first issue is the supported catalysts; the second, the self-supported or unsupported catalysts and finally, a brief discussion about the theoretical studies. We also inspect some details about the effect of support, the use of organic and inorganic additives and aspects related to the preparation of unsupported catalysts. We discuss some hot topics and details of the unsupported catalyst preparation that could influence the sulfur removal capacity of specific systems. Parameters such as surface acidity, dispersion, morphological changes of the active phases, and the promotion effect are the common factors discussed in the vast majority of present-day research. We conclude from this review that hydrodesulfurization performance of TMS catalysts supported or unsupported may be improved by using new methodologies, both experimental and theoretical, to fulfill the societal needs of ultra-low sulfur fuels, which more stringent future regulations will require.

**Keywords:** hydrotreating; CoMo; NiMo; NiW; CoW; hydrodesulfurization; sulfur removal; molybdenum sulfide; tungsten sulfide; support effect; unsupported catalysts; promoter; ultra low sulfur diesel; density functional theory

## 1. Introduction

Currently, the refining processes for purifying petroleum products have experienced significant growth in the production volume due to the constant increase in global fuel consumption. Gasoline consumption is expected to be growing almost 1% per year whereas the ultra-low sulfur diesel (ULSD) demand is expected to grow closer to 2% per year [1].

To fulfill this increasing demand, the refineries must process heavier petroleum fractions feedstocks. The processing of heavy oils presents a complex problem since it requires pressure and temperature increases to meet the particular requirements to remove sulfur from refractory compounds [2]. Coupled with this, the environmental regulations have been changed to historically lower levels [3]. In Europe and the USA, the sulfur content limits are now between 10 to 50 ppm for gasoline and diesel [4]. Besides the “zero sulfur” emissions are targeted shortly around the globe [5–7]. The drastic decrease in the sulfur-containing compounds in gasoline and diesel specifications have led to the development of

more active and selective catalysts. However, this deep level of hydrodesulfurization (HDS) requires a significant increase in the relative volume activity [8]. The problem at this moment is that most of the available information about this process and the involved catalysts has been acquired focusing on desulfurizing light petroleum fractions.

Sulfur content in crude oil varies widely between regions and countries, i.e., from 0.1 wt. % for North African and Indonesian [9] to 6.0 wt. % [10] recently reported for the Mexican Altamira heavy crude oil. Besides, high sulfur heavier oils are increasingly used because the worldwide light crude reserves are drastically decreasing or even reaching depletion see Figure 1. This emerging need to process heavy crude oil fractions currently drives both refineries and academic research.

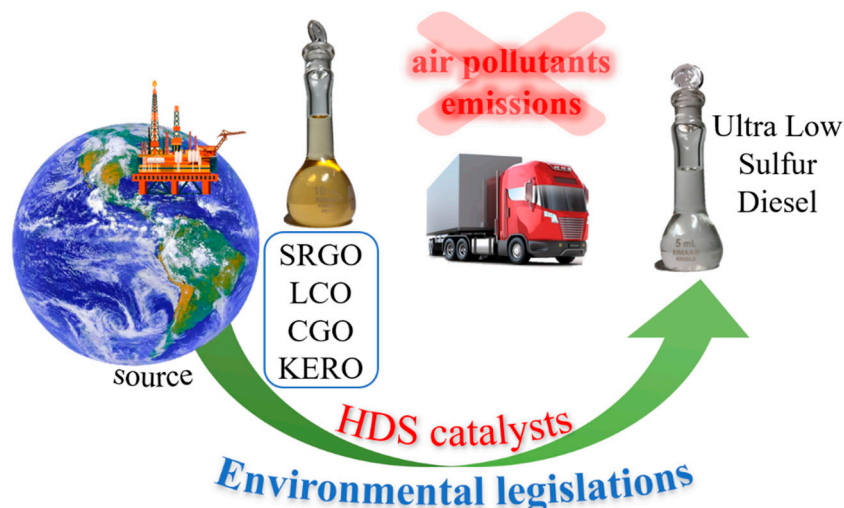


**Figure 1.** Impacts on ultra-low sulfur diesel production.

The refineries are presently not prepared to process heavy fractions and treating them represents a major operational and economic challenge for industry [5]. On the one hand, the complexity and quantity of sulfur compounds to be hydrotreated in the bulk fractions are considerably larger than in those where the actual HDS units are dispersed. For example, in the 90s, one unit that was designed to produce a targeted diesel with 1500–350 ppm S; now, the same unit has to produce <10 ppm S ULSD without sacrificing production and achieving API (American petroleum institute) uplift in the diesel product. On the other hand, the so-called ultra-deep hydrodesulfurization is needed to reach the sulfur content limits (present and future) [11–13]. Therefore, highly active catalysts seem to be the critical factor to deal with the bulk sulfur compounds and remove them selectively from refractory alkyl-substituted dibenzothiophene (DBT) molecules such as 4,6 dimethyl DBT (4,6-DM-DBT), 4-methyl 6-ethyl DBT (4M,6E-DBT), 4,6 dibutyl DBT (4,6-DB-DBT), or 4,6 dipropyl DBT (4,6-DP-DBT) [5,14].

Sulfur removal from sterically hindered compounds presents a strong inhibition effect of polyaromatics and nitrogen-containing compounds, which must be solved at the same time [15]. To overcome these problems, the HDS units need to increase their working pressure and temperature conditions; however, this carries along another series of problems [16]. Coke deposition and gradual segregation of the active phases may be observed in the long-term if the working catalyst loss stability.

Other options, such as revamping the hydrotreating units or building new ones may be considered, and the economic cost could be very high but affordable [5]. For example, the previously mentioned unit designed in the 1990s to produce a targeted diesel with 1500–350 ppm S but now must produce <10 ppm S ULSD without sacrificing production and achieving API uplift in the diesel product would certainly need revamping. An estimation by the Environmental Protection Agency (EPA) for installing a new HDS unit at a place in the refinery to obtain ULSD of 15 ppm S or less would cost twice the price than that to obtain low sulfur diesel (500 ppm of S) [17,18].

The literature dealing with hydrodesulfurization catalysts to produce ULSD is wide and vast. Different research lines are well defined and followed by specific investigation groups [19]. Also, a wide variety of advanced techniques have been used to explain the structure, dispersion, promotion, morphology, and activity of HDS catalysts [20]. Despite the difficulty of splitting all related literature into groups, we will divide this review into three broad areas, i.e., supported catalysts, unsupported catalysts, and related theoretical studies.

## 2. Supported HDS Catalysts

### 2.1. The Role of Support in the Active Sulfide Phases

The nature of the support generally plays a key role in the morphology, dispersion, and obviously in the catalytic activity of the prepared catalysts [21,22]. Besides, it is well known that conventional alumina is not a totally inert carrier under reaction conditions and could allow the migration of the active promoters, such as Co or Ni, into its more external surface forming sub-superficial spinels [23] or promote isomerization reactions depending on the acidic character of those ions. In early reports, Topsøe et al. recognized that if the interaction between the CoMoS phases and the alumina carrier can be eliminated or at least considerably decreased, the new sulfided structures would have more intrinsic activity [24,25]. This fact allowed them to propose the existence of a different structure with lesser support interaction, which they called CoMoS phase type II. Since then, much research has been done trying to modulate the support interaction with the active phases. It is currently well accepted that catalysts for different oil fractions must present slight differences related to the metal support interactions. Therefore, modulation of the active phase dispersion over alumina is the determining factor of activity, selectivity, and stability (see Figure 2) [16].

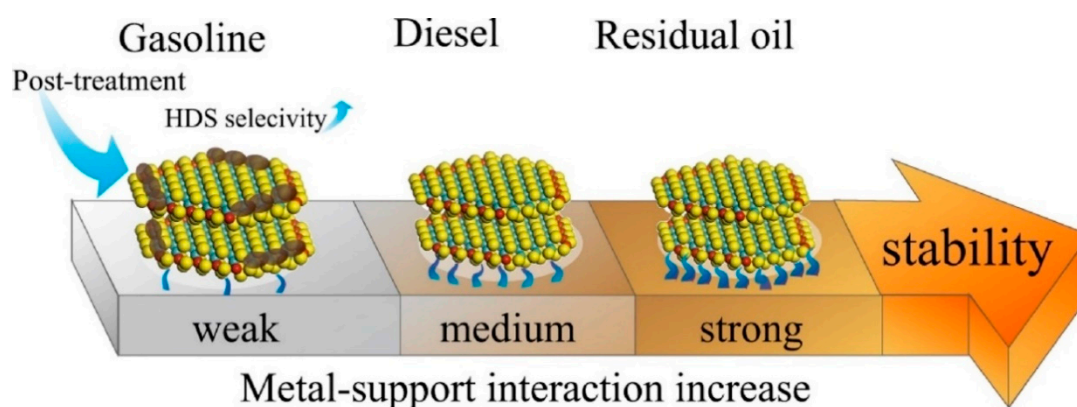


**Figure 2.** Metal-support interactions in hydrotreating catalysts depending on the intended use by H. Nie et al. [16].

In this sense, understanding the effect of the support has been extensively pursued. The dispersion, average stacking, and length of the MoS<sub>2</sub> or WS<sub>2</sub> slabs and the way in which metal sulfides are bonded to the support surface are the focus of several investigations [26]. Early reports mentioned that the catalytic performance of MoS<sub>2</sub>-based catalysts strongly depends on their morphology but also on the orientation, since slabs may be bonded either by the edge or by the basal planes [27] depending on the support. Usually, over gamma alumina, the preferential bonding is by the basal planes (111) and (100) since these display relatively weak and intermediate interactions with MoS<sub>2</sub> structures respectively as Bara et al. recently showed [28]. By contrary, the plane (110) presented highly dispersed and oriented oxide particles with strong metal support interaction, the authors associated this plane with small and weakly stacked MoS<sub>2</sub> slabs and a very low sulfidation degree.

Sakashita et al. provided the evidence of MoS<sub>2</sub> clusters bonded to TiO<sub>2</sub> anatase surface by the edge planes [29]. Transmission electron micrographs clearly showed the (002) plane of the MoS<sub>2</sub> clusters with 0.6 nm of interplanar spacing see Figure 3.

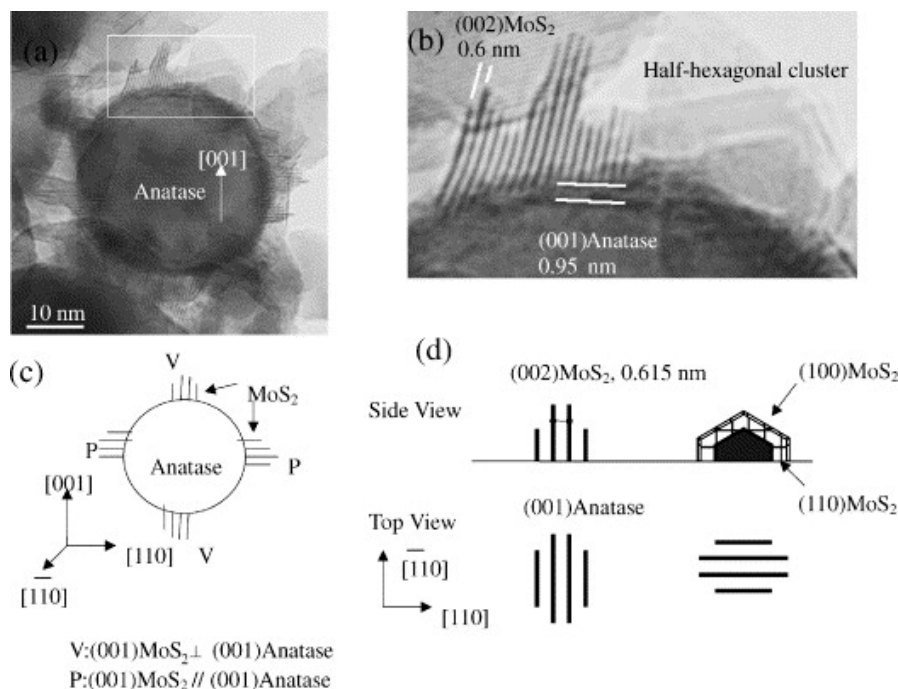


**Figure 3.** (a,b) TEM micrographs and (c,d) schematic diagrams of MoS<sub>2</sub> clusters supported on TiO<sub>2</sub> anatase powders. Sakashita et al. [29].

Some years later, Arrouvel et al. using density functional theory (DFT) calculations confirmed that the anatase surface could enhance tilted and perpendicular orientations for the MoS<sub>2</sub> cluster due to epitaxial growth. Also, they proposed that the (110) plane of hydroxylated alumina could allow a slab tilted orientation due to the flexibility of its hydroxyl groups [30]. Recently, it was proposed that an excess of superficial Al with respect to stoichiometric one, due to the morphology of the support, could also lead to slab-orientations effects [31]. During the preparation of the surface oxides, Me–O–Al linkages are formed, which allows the later formation of WS<sub>2</sub> crystallites bonded through their high energy edge planes to the alumina surface. The formation of W–S–Al bonds allows the WS<sub>2</sub> crystallites to be anchored to the surface at angles close to 90° [32]. Recently, Berhaut discussed that the edge-basal plane ratio and the particle size along the axis of the MoS<sub>2</sub> particles influence the catalytic behavior [33]. Studies by his group pointed out that also in the basal planes could be created active sites when the slabs present some bending [34].

Nevertheless, to directly observe the entire active phase and isolate the bending effects involves a great challenge. As Berhaut pointed out, the disordered state of molybdenum sulfide, the dispersion and the fact that only 10% of the active phase is actually observed by transmission electron microscopy (TEM) due to the orientation of the slabs contribute to this difficulty. Díaz de León et al. recently published a study of the effects of support on NiW catalysts. They detected the presence of slabs which have some bend in almost all samples analyzed by high resolution transmission electron microscopy (HRTEM) [4]. The mentioned bend was more clearly observed in the NiW catalysts prepared over Al<sub>2</sub>O<sub>3</sub>–TiO<sub>2</sub> (AT) and ZrO<sub>2</sub>–TiO<sub>2</sub> (ZT) mixed oxides. To elucidate this and other related effects, a systematic experimental-theoretical study was conducted using  $\gamma$ -Al<sub>2</sub>O<sub>3</sub> (A), SiO<sub>2</sub> (S), TiO<sub>2</sub> (T), ZrO<sub>2</sub> (Z), AT, and ZT as supports to synthesize NiW catalysts with the same atomic density per square nm [35]. They proposed that the metal-support interaction may be modulated by substituting the carrier and that specific interaction is directly observed in the slab length and stacking of the active

phase. Interestingly, they found that the mixed oxides ZT and AT showed the highest activities among the series. Their DFT results revealed that the promoted slabs tend to be bent by the interaction with the support due to a charge redistribution that induces a loss in crystallinity and creates defects with high hydrogenation capacity all over the slabs in the inflection points [35], as Shimada and his group had previously pointed out [36]. In this context, Afanasiev recently prepared hollow metal sulfide nanoparticles to analyze the slab curvature effect (see Figure 4) [37]. He evidenced a significant number of defects in the hollow MoS<sub>2</sub> nanospheres due to dislocation of planes (002) at the joint points. His results showed significant evidence of the contribution to the catalytic activity of the slab curved basal planes of the slab. Finally, he also proposed that for chemically similar supports, a higher curvature of MoS<sub>2</sub> particles might have an advantage over a less curved counterpart [37].

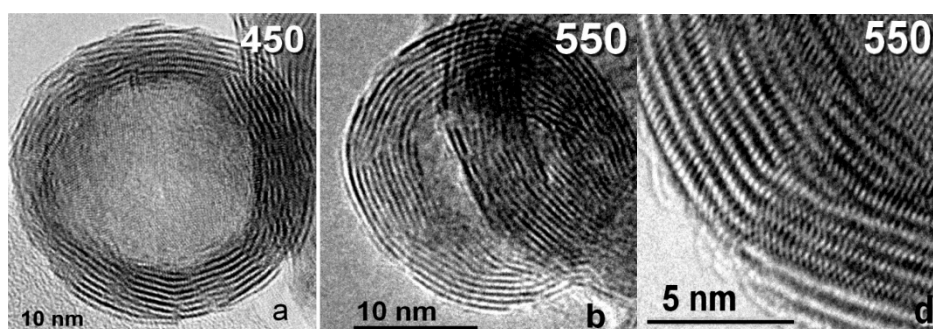


**Figure 4.** Taken and modified from [37], high resolution transmission electron microscopy (HRTEM) images of hollow spheres prepared by P. Afanasiev.

#### Mixed Oxides Support: A Different Approach

As mentioned earlier, the research directed to modulate the metal-support interaction can be envisaged from many viewpoints, such as the use of crystallographic phases different from the typical gamma alumina [38] or supporting the active phases over unconventional single metal (M<sub>s</sub>) oxides such as those based on Ti [26,39–45], Zr [26,41–44,46,47], Si [23,26,48–50] or Ga [51]. Nevertheless, more recently to gain advantage from the individual single metal oxide properties and to overcome their intrinsic limitations, several binary mixed oxide materials such as Al<sub>2</sub>O<sub>3</sub>–Ga<sub>2</sub>O<sub>3</sub> [50], Al<sub>2</sub>O<sub>3</sub>–TiO<sub>2</sub> [4,52–57], ZrO<sub>2</sub>–TiO<sub>2</sub> [35,58,59], Al<sub>2</sub>O<sub>3</sub>–ZrO<sub>2</sub> [60–62], MgO–TiO<sub>2</sub> [63], Al<sub>2</sub>O<sub>3</sub>–MgO [56,64], Mn–Al<sub>2</sub>O<sub>3</sub> [65–67], and Al<sub>2</sub>O<sub>3</sub>–zeolite [68] have been studied, among several others that have been tested to prepare HDS catalysts. As expected, in several cases higher activities of catalysts prepared over those mixed oxides were reported compared with those supported on alumina. Modifications of the morphological parameters such as length and stacking of the MoS<sub>2</sub> slabs prove that the interactions can be modulated. A few authors have also reported clear differences between support properties such as surface acidity, surface area, surface potential and electronic properties, among others.

Nevertheless, structure-activity correlations have not been clearly stated yet, and the exact composition of each support participating in the new mixed oxide always plays a role in the final observed catalytic properties. Early studies showed for example that Mo over Al/Ti = 1 and Ti/(Ti + Zr) = 0.8 supports lead to the highest activities among tested catalysts for hydrocracking and coal-derived liquids upgrading [69]. For the HDS of DBT, several reports have been published using Al/Ti = 2 to obtain the highest activity [4,35,52,55] among materials prepared by the sol-gel method.

In all cases, the precursors and the methodology to mix the catalysts also impact the activity results [70,71]. Recently, our research group reported that for NiW, the effect of support could be elucidated by unraveling how the sulfide cluster interacts with the surface [4,35]. Normally, when a catalyst (NiMo, CoMo, or NiW) is synthesized, the metal–O–M<sub>s</sub> linkages are expected to be formed (M<sub>s</sub> refers to the metal in the support). During the sulfiding process, these Mo–O–M<sub>s</sub> bonds are broken and transformed into Mo–S–M<sub>s</sub> bonds. Nevertheless, some of these Mo–O–M<sub>s</sub> bonds could remain at the periphery of the MoS<sub>2</sub> slabs [72]. When the Mo–S bonds are formed, the interaction between

the metal sulfide slab and the support can be redefined and could be calculated through DFT. These results also indicated that in Ti-containing supports the orientation effects of metal sulfide slabs were clearly observed, although in the mixed oxide the cluster seems to have more affinity to Al or Zr than to Ti. Therefore, when clusters “avoid” having contact with specific atoms on the surface, the cluster tends to be bend. This slab-bending effect should be carefully analyzed under the light of the recent findings discussed in the previous section.

## 2.2. Details of ULSD Catalyst Preparation

The supported catalysts for industrial application are typically prepared by incipient wetness impregnation of the metal precursors over hot alumina pellets. By adding organic or inorganic additives to the  $\text{Al}_2\text{O}_3$  based catalysts, their activity can be modulated. Consequently, the additives prevent the migration effect and thus increase the participation of promoter-atoms in the formation of the nonstoichiometric CoMoS phase through the S-edges of  $\text{MoS}_2$  [73]. Therefore, the concentration, temperature of the solution and especially the pH of the solutions strongly affect the species in the aqueous solutions and their interaction with the carrier surface. The metal hydroxide species involved in the mother solutions (at a specific concentration and pH) for the preparation of catalysts could be cationic as in  $[\text{Ni}(\text{H}_2\text{O})_6]^{2+}$  species [74] or anionic as in  $\text{Mo}_7\text{O}_{24}^{6-}$ ,  $\text{MoO}_4^{2-}$  [75],  $\text{HW}_6\text{O}_2^{15-}$ , and  $\text{W}_6\text{O}_2^{16-}$  species [76] at the same pH. The electrostatic interaction of these species with the support surface depends on whether the surface is positively or negatively charged at the defined pH. Alumina has a zero point of charge (ZPC) at pH of about 8, so above this value, its surface is negatively charged. Meanwhile, below that pH value, the surface is positively charged [75]. Díaz de León et al. stated that a change in the surface potential could induce a modification in the species deposited over the surface. Their Raman spectroscopy results showed that the ratio between (O = W = O + W = O) terminal bonds and the internal W–O–W bonds changed depending on the surface potential of the support materials [76]. Also, Vazquez-Garrido et al. attributed the differences in the Mo oxide surface species to the differences in the Z potential of their supports (for  $\text{Al}_2\text{O}_3$ –MgO it was 9.0 while for the  $\text{Al}_2\text{O}_3$ – $\text{TiO}_2$  4.9). For the  $\text{Al}_2\text{O}_3$ – $\text{TiO}_2$  support, the species obtained were  $\text{Mo}_7\text{O}_{24}^{6-}$  and  $\text{Mo}_8\text{O}_{26}^{4-}$ , while for the basic support it was  $\text{MoO}_4^{2-}$  [57].

### 2.2.1. Organic Additives

As we mentioned, during the preparation of hydrodesulfurization catalysts is possible to include precursors of the active phases as Mo or W, promoter atoms such as Co or Ni as well as additives. Nevertheless, the preparation of the CoMoS, NiMoS, or NiWS mixed sulfide phases is of paramount importance and have to be maximized for attaining the highest possible activity. In that sense, the use of chelating agents has proven to be a very useful route to prepare highly active HDS catalysts. The first effect of chelating agents is that they can form complexes with the Co, Ni, Mo, or W precursors that change the coordination sphere of this metals and avoid the later formation of isolated ions over the surface of support increasing the participation of promoter ions in the nonstoichiometric Co(Ni)Mo(W)S phases. The second known effect is a delay in the sulfidation process [76–78] avoiding the consequent segregation of the thermodynamically stable Co or Ni sulfides ( $\text{Co}_9\text{S}_8$  or  $\text{Ni}_3\text{S}_2$ ). It is well known that cobalt oxide sulfidation takes place at a much lower temperature than for tungsten oxide. However, only a few reports are available on the segregation effect during the sulfidation process as for Co-W sulfide catalysts [79,80]. Vissenberg et al. showed that 473 K is enough temperature to obtain a high quantity of stable  $\text{Co}_9\text{S}_8$ . They also pointed out that, as soon as  $\text{WS}_2$  is formed, the  $\text{NiS}_x$  particles re-disperse to form the NiWS phase [81]. Meanwhile, the  $\text{CoS}_x$  particles continue forming more  $\text{Co}_9\text{S}_8$  instead of the CoWS phase.

Some authors have suggested that the use of chelating agents could solve this problem. Kishan et al. successfully used 1,2-cyclohexanediamine-*N,N,N,N*-tetraacetic acid (CyDTA) and triethylene-tetraaminehexaacetic acid (TTHA) during the impregnation procedure, obtaining circa 2.4 times more activity for CoW catalysts prepared with TTHA than for catalysts prepared without

chelating agents [82]. Nevertheless, the lower activity displayed by this combination in comparison with NiW, NiMo, and CoMo has discouraged the study of this system.

Saccharose (SA) was also used as an organic additive in simultaneous impregnation of NiMoP/Al<sub>2</sub>O<sub>3</sub> preparation [83]. Authors observed a significant improvement in the dispersion of metallic species, increases in the sulfurability of Ni oxide species and the catalytic activity at low SA content inclusions. However, increasing the SA leads to an increase in the carbon content, which induces a severe blockage of the active sites. Studies using nitrilotriacetic acid, ethylenediamine, ethylenediaminetetraacetic acid (EDTA) have shown favorable effects enabling the formation of the active phase, and this increases the activity [77,84–86]. Recently, hydrocarboxylic acids have been shown to induce higher catalytic behavior than catalysts prepared using amino polycarboxylic acids [87]. Among them, citric acid (CA) has attracted widespread attention when used to prepare promoted catalysts such as CoMo, NiMo, or NiW systems due to its low cost and excellent solubility. Several authors have reported that CA could be able to improve the dispersion of Mo (W) [88–92], modify the morphology of the MoS<sub>2</sub> slabs [93,94], change the excessive metal support interaction [73,89,95–97] and help to delay the sulfidation process [73]. Likewise, there is a consensus that CA improves the promotion effect of Co or Ni atoms and therefore increases the participation of the promoter atoms in the formation of the mixed Co(Ni)–Mo–(W)–S phase.

As mentioned before, the pH of the impregnation solutions could also determine the morphology of the active species. Studies by D. Valencia et al. using different pH values to prepare NiMo catalysts and adding CA, confirmed that the pH of the impregnation solution is determinant of activity and selectivity [98–100]. Also, the authors reported that an increased amount of CA during the synthesis improved their NiMo catalysts in the direct desulfurization pathway. Later, Castillo-Villalón et al. reported that the incorporation on CA modifies the morphology of MoS<sub>2</sub> crystallites [101]. Their results suggested that CA increases the formation of Mo–S sites at the S-edge of the slabs. Similar results were simultaneously published by J. Chen et al. [94]: by using infrared spectroscopy the authors found that CA promoted the growth of the S-edge of MoS<sub>2</sub> slabs, gradually changing the morphology from a slightly truncated triangle with predominately M-edge to a hexagon with more or less the same size proportion of M-edges and S-edges, as shown in Figure 5.

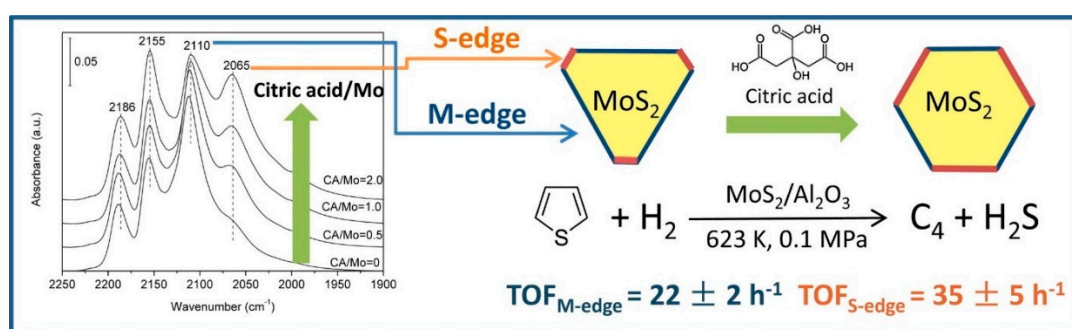


Figure 5. Effect of citric acid in slabs morphology, J. Chen et al. [94].

Additionally, Suarez-Toriello et al. showed that CA could induce isolation of impregnated metal species avoiding excessive metal-support interactions and delaying nickel reduction at higher temperatures. The authors found that CA incorporation prevents the formation of insoluble nickel species and soluble Ni–Cit-species are formed instead. Their XPS and activity results also suggest that this effect is directly reflected as an increase of Ni participation in the formation of the nonstoichiometric NiWS phase [74].

It is well known that the lifetime of a catalyst in an industrial hydrotreater strongly depends on the operating conditions and the liquid feed quality. HDS catalysts deactivate with time due to coke deposition, sintering, or metal poisoning among other contaminants [102]. Dufresne suggested that some oxygen compounds can act as redispersion metal agents when a decoked catalyst is being

reactivated [102]. In that sense, chelating agents have also been used to control the regeneration of wasted catalysts with promising results. Maleic acid was used by Bui et al. [103] to regenerate CoMo catalysts. Their results showed that this chelating agent is capable of extracting Co from CoMoO<sub>4</sub> species efficiently and form a cobalt maleate complex. This complex releases the Co after 300 °C favoring the redecoration of the MoS<sub>2</sub> slabs and increasing the activity.

Pimerzin et al. [104] also used different organic additives as CA, ethylene glycol (EG), tri-ethylene glycol (TEG), thioglycolic acid (TGA), and dimethylsulfoxide (DMSO) to treat spent CoMo catalysts, finding similar results as Bui et al. [103]. The authors found that the use of CA, EG, TEG, or TGA restore almost entirely the catalytic activity due to the redispersion of active metals allowing the formation of new highly promoted active CoMoS phase. Another study performed by Zhang et al. using CA to modify CoMo/ $\gamma$ -Al<sub>2</sub>O<sub>3</sub> calcined catalysts revealed that the sulfidation degree of the MoO<sub>x</sub> species and the activity of the CoMo catalysts linearly increased with the CA applied [105]. These authors also proposed that the MoO<sub>4</sub><sup>2-</sup> or  $\beta$ -CoMoO<sub>4</sub> species can be successfully transformed into polymolybdate species. Finally, the addition of CA can also help to recover Co<sup>2+</sup> ions from the sub-superficial CoAl<sub>2</sub>O<sub>4</sub> spinels and, therefore, to induce the formation of more CoMoS sites.

### 2.2.2. Inorganic Additives

As mentioned in the previous section, the chelating agents are usually introduced into the system in an attempt to avoid the loss of the promoter atoms in the sub-superficial layers of supports. This effect leads to the direct interaction of Ni hydroxide cations (or Co) with the cation deficient octahedral or tetrahedral sites at the more external layers of the metal oxide surface. When this migration phenomenon happens, some part of the promoter charged to the catalysts is lost in the formation of sub-superficial spinels.

The introduction of additives such as F [106,107], Mg [108–111], B [112–116], P [86,117–119], or Ga [76,120–124] seems to correctly solve the migration phenomena, and to improve stability and lower the interaction between the active phase and the support. Nevertheless, other aspects, such as activity and selectivity should be carefully observed, since the surface and textural properties sometimes change drastically, and in most of the cases, large increases in the additive content, in fact, cause a decrease in activity [76,118].

Typically, due to the nature of the additives, changes in surface acidity are reported [76,106,112]. For example, F, Mg, B, and Ga regulate the Bronsted acidity leading to changes in the electronic properties of MoS<sub>2</sub> and CoMoS sites, whether these changes affect or not the morphology of the sulfide phase [106,109,114,125]. In particular, Ga used as an additive of alumina support, modifies the general morphology of WS<sub>2</sub> slabs by changing the dispersion and increasing the promotion of the active phase almost to the maximum theoretical Ni promotion ratio [120]. These findings revealed that the formation of GaAl<sub>2</sub>O<sub>4</sub> over the surface not only changes the surface potential compared with the original alumina but also inhibits the Ni migration phenomena. Besides, as a natural consequence, the quantity of Ni in octahedral species (Ni<sub>oct</sub><sup>2+</sup>) related to the promotion of the active phase [126] increased considerably. The effect of additives is generally observed directly on the activity and selectivity. In this sense, the hydrogenation pathway seems to be more sensitive to the inclusion of additives. Han et al. found that the inclusion of F in the MoS<sub>2</sub>/Al<sub>2</sub>O<sub>3</sub> system can have a substantial effect on the Bronsted acidity [107]. They proposed that the Bronsted sites interact with the active phases in the surroundings allowing an induction effect that leads to an electron deficient state increasing the formation of coordinatively unsaturated sites (CUS), which raise the hydrogenation capacity.

Moreover, the hydrogenation pathway is expected to proceed via the  $\pi$ -bonds due to steric hindrance effects of alkyl substituents. The so-called BRIM sites, when present, are associated with increases in the hydrogenation capacity [127]. Therefore, it may be suggested that the presence of additives induces an increase in the local metallic character of the Ni–Mo(W)–S edge sites, in the phases allocated in the neighborhood of these additive metals. Particle size could also cause a modification in the metallic character of the NiWS edge sites [30], and as mentioned, the inclusion of additives induces

increases in the dispersion of the active phase. Therefore, the change in slab size could by itself explain modifications in the selectivity.

### 2.3. Concluding Remarks

The hydrodesulfurization activity of the supported catalysts depends upon several factors: type of support, active component, organic-inorganic additive, and their content, pH of the impregnation solution, metal-support interaction, type of promoter and its content, slab length-stack number and sulfidation conditions such as temperature and time among others. Furthermore, inorganic-inorganic additives improve the thermal stability, can modulate the metal support interactions, dispersion of metal sulfides, acidity and could generate the CUS in the catalyst. By keeping all these factors in mind, a catalyst, which surely will produce ultra-low sulfur fuels can be designed.

## 3. Unsupported HDS Catalysts and Their Structure-Activity Relationship

Unsupported catalysts have received much attention in recent years due to their high activity about 2.5–3 times higher than for supported catalysts and because of the stringent environmental legislation obliging refineries to produce ultra-low sulfur fuels. Unsupported catalysts can be used as a whole and as one of the layers (20–30% of reactor load) in commercial scale reactors to produce ULSD. The present section deals with the structure-activity relationship studies of unsupported catalysts. Unlike the supported catalysts, no metal support interactions (strong and weak) are present for the self-supported catalysts. However, the metal sulfide slab length and stacking determine the activity of catalysts which depends on the synthesis procedure. Therefore, the catalyst synthesis method is essential, with that in mind this section is further divided into two subsections, namely the direct synthesis of metal sulfides by the decomposition method and the synthesis of the metal oxide precursors followed by in-situ/ex-situ sulfidation.

### 3.1. Decomposition of Thiosalts

This section describes the structure-activity relationship of promoted and un-promoted bulk MoS<sub>2</sub> catalysts derived from the decomposition of precursors such as thio-salts [128–130], an alkyl group-containing salts [131–134] and oxythiosalts [135,136], and others. Various factors associated with the catalyst performance and their effect on HDS activity and selective path (hydrogenation (HYD) or direct desulfurization (DDS)) have been reported in the literature, these include, the effect of carbon, promoter effect, transition metal sulfides, catalyst activation temperature, use of activation gas, and synthesis methods.

The hydrodesulfurization activity of catalysts prepared from decomposition depends upon the content of promoter, temperature and activation gas (hydrogen or nitrogen) used, which in turn could determine the number of layers, length of the slabs and slab orientation. For example, the Ni promoted catalysts (NiMo or NiW) prepared under hydrogen environment and at high temperatures exhibited high activity [128,135] and normally displayed a combination of short slab lengths and low stacking degree. Besides, the catalyst in which a low stacking degree was detected along with curved slabs [128], resulted in high activity [131] as reported by Nogueira et al. [34] and Afanasiev [37] due to the presence of defects in the slabs as we discussed in Section 2.1. Similar results were observed for CoMo catalysts activated under hydrogen atmosphere displaying small MoS<sub>2</sub> slabs with low stacking number and higher activity (through DDS route) compared to the catalyst activated under nitrogen environment [129].

The major drawbacks of the unsupported catalysts are typically low surface areas, lower dispersion of slabs and longer slab lengths. Therefore, in order to overcome these problems and improve the catalytic performance further, some research groups utilized organic surfactants [136] and alkyl containing precursors [131–134] (as the alkyl group acts as an internal template) that can improve the dispersion of the metal sulfide slabs and higher surface areas during the synthesis of catalysts. In that sense, Acuña et al. synthesized tri-metallic catalysts (CoMoW) with various carbon chain lengths from

C<sub>1</sub> to C<sub>3</sub>. They observed that with the increase in the alkyl chain length the organic carbon increased considerably, and this was directly reflected on the BET surface area showing increments. However, it was not observed a significant change in the catalytic activity that could be attributed to the alkyl chain [132]. Authors reported that the major drawback of the alkyl-containing precursor was the formation of char during the decomposition process. This carbon blocked the active sites, therefore, playing a negative role in HDS activity. Besides, they observed that the increase in alkyl chain of the precursors showed impact on the slabs length decreasing it, but no influence on the stacking degree was observed. Contrariwise, a positive effect of carbon was observed for unsupported catalysts by Armenta et al. for the same combination of trimetallic catalyst (CoMoW) but using carbon chain larger than what Acuña et al. reported [132]. The authors used chains from C<sub>12</sub> to C<sub>18</sub> observing the formation of sulfur carbide. In this case, the carbon formed during the decomposition of precursors served as dispersing agent [133]. Besides, the HDS activity results showed that the DDS route was the main reaction pathway and was dependent on the carbon content in the final catalysts. Romero et al. also reported similar observations for MoS<sub>2</sub> catalysts, as the activity of the catalyst, was proportional to alkyl chain length up to certain extent above which it acts as a poison for the catalyst due to active sites were covered by carbon [134]. Moreover, the favored catalysts mechanism was through the hydrogenation path.

The type of promoter and its loading in the catalyst has a significant effect on the degree of sulfidation of metal oxides which decides the HYD or DDS mechanism and tolerance to the heterocyclic compounds present in the real feed [137]. Metal sulfides like MoS<sub>2</sub> and WS<sub>2</sub> are known to be active in HDS. However, the HDS performance of the un-promoted catalysts depends upon the type of the feed. The studies on hydrogen index and hydrodesulfurization on model compounds reported by Ho et al. indicated that MoS<sub>2</sub> exhibited high activity for model compound and poor performance in the case of real feed. The authors claimed that this was due to an intrinsic (hydrogenation) and an environmental factor (tolerance to organo-nitrogen). Introduction of Co, in MoS<sub>2</sub> resulted in high activity for the real feed indicating the importance of the promoter. Various promoters such as Co, Ni, or Fe have been used for MoS<sub>2</sub> unsupported catalysts [138]. The authors observed a higher sulfidation degree when the promoter used was Ni. This is in agreement with the results reported by Le et al. in the case of NiW unsupported catalysts. These authors observed that the sulfidation degree increased almost linearly with the increase in the Ni wt. % content [135]. On the other hand, Yi et al. observed that increasing the Ni content in the catalyst results in low stacking of Mo/WS<sub>2</sub>, which in turn exhibited low activity [139].

Moreover, the promoter content determines the catalyst mechanism whether reaction proceeds through HYD or DDS route. High loadings of promoter content increase the hydrogenation (HYD route) and vice versa (Bocarando et al.) [140]. Apart from the role of promoters, metal additives like Ga could generate coordinatively unsaturated sites in the catalysts as reported by Zepeda et al. [141].

Another fact that some researchers have studied is the metal-sulfur bond energies [142] and their role over the stoichiometric sulfur located at the edge in MoS<sub>2</sub> slabs [143]. For example, Daudin et al. [142] reported a study about various transition metal sulfides where they found a direct correlation between the HDS/HYD selectivity and the metal-sulfur bond energies, as shown in Figure 6. They proposed three cases: when metals presented low (1) and high (2) sulfur-metal bond energies exhibited high activity for the hydrogenation route. While when they presented moderate (3) metal-sulfur bond energy, the DDS increased rapidly exhibiting the highest HDS/HYD ratio among the studied systems. Moreover, the authors found an almost perfect fit for their experimental results using Langmuir-Hinshelwood kinetics. They proposed that the dissociation of H<sub>2</sub>S and H<sub>2</sub> takes place on Me-S (metal-sulfur) species and free metallic sites while the competitive adsorption of the organosulfur molecules and alkenes occurs only on the metallic sites.

Afanasiev et al. observed that stoichiometric sulfur (S<sub>2</sub><sup>2-</sup> species) present at the edges of unsupported MoS<sub>2</sub> slabs plays a key role in the catalytic activity [143]. The -SH groups produced from the S<sub>2</sub><sup>2-</sup> species by the interaction with hydrogen have a strong impact on the catalytic behavior. The catalysts presenting this effect controlled the HDS reaction through the HYD route. The affinity of

nickel and cobalt ions toward the MoS<sub>2</sub> slabs at the sulfur edge resulted lower than when –SH groups appear at the edges.

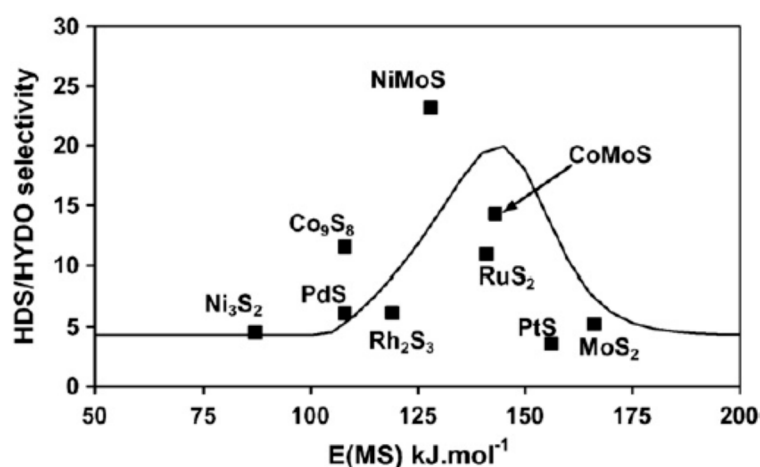


**Figure 6.** Selectivity hydrodesulfurization, comparison between experimental results and kinetic model (black line) as a function of sulfur–metal bond energies,  $E(MS)$  ( $T = 250$  °C,  $P = 20$  bar,  $H_2/$ feed = 360 l/l). Daudin et al. [142].

### 3.2. Oxides Followed by Sulfidation

#### 3.2.1. Template-Free Method

In the case of catalysts prepared through synthesis by template-free method of an oxide catalysts and followed by thermal sulfidation process, we focused the discussion on three synthesis procedures as follows: (i) layered double hydroxides [144–147]; (ii) hydrothermal method [148–151]; and (iii) precipitation method [152,153]. Layered double hydroxides (LDH) are used as precursors and structural templates as well for the synthesis of HDS catalysts [147]. The activity of catalysts derived from the LDHs are dependent on the geometric position of the hexavalent metal ions in tetrahedral or in octahedral coordination [144], the surface area of the precursor oxides, promoter content, activation temperatures, etc. Similar properties were observed for catalysts derived from thiosalts and LDHs. However, the activation temperatures are relatively high especially in the case of W containing catalysts derived from LDHs [146] when compared to catalyst derived from thio-salts. Moreover, Coelho et al. observed that there was no correlation between the activity of catalysts derived from LDHs and properties such as the surface area or the Mo/Al ratio [145].

In order to achieve high surface areas for the unsupported catalysts, the hydrothermal method was also adopted for the catalyst synthesis. It is known that the catalytic activity of catalysts is strongly proportional to catalyst activation temperature which in turn depends on variation in catalytic properties like crystalline nature, defects in basal planes, size-shape, agglomeration of metal sulfides [148,149]. Yin et al. observed that an increase in sulfiding temperature resulted in agglomeration of Ni<sub>3</sub>S<sub>2</sub> and MoS<sub>2</sub>/WS<sub>2</sub> nanoparticles and increases the stack of MoS<sub>2</sub>/WS<sub>2</sub> [148]. Similar results observed by Zhang et al. [149]. The increase of sulfidation temperatures results in crystallinity of the MoS<sub>2</sub>, longer slabs, and showed curved shape. Additionally, it was reported that the formation of defects on the basal planes acts as active sites with high activity in HDS as we discussed in Section 2.1. Also in some of the studies, it was reported that the presence of Lewis acidic sites resulted in de-alkylation [150] and isomerization reaction [151] in the case of alkyl-substituted DBTs.

Other effects have also been studied such as the use of non-conventional promoters, the use of metals such as Zn or Cu [152,153] as additives as well the use of solvents synthesis [154,155] or the inhibition effect of imparted by the nitrogen-containing compounds [156] on unsupported catalysts preparation. Nevertheless, some of these parameters use to exhibit great impact on the HDS catalytic activity changing the sulfidation degree or modifying the particles sizes. For example, Yue et al. [154]

achieved smaller catalyst particles when a methanol-water mixture was used for the unsupported catalyst synthesis. It was observed that the improvement in catalytic properties is related to the increase in the sulfidation degree and to the high dispersion of the active components. Also, the authors found a direct correlation between the DBT conversion and the weakly bonded sulfur on the catalyst surface (Figure 7).

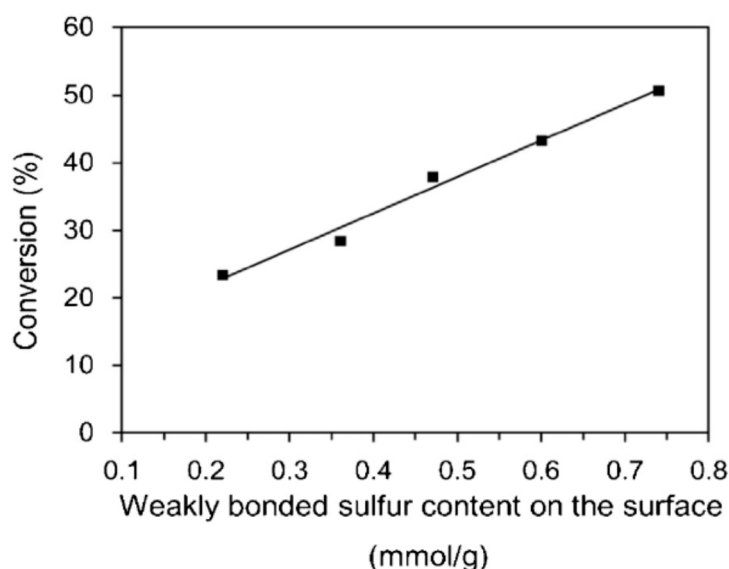


**Figure 7.** The relationship between the DBT conversion and weakly bonded S content of the catalyst. Yue et al. [154].

### 3.2.2. Template Method

Another method for achieving high surface areas and improve the dispersion is the use of organic templates. This section deals with the hydrodesulfurization activity of the catalysts synthesized using various organic templates such as polyethylene glycol [157–160], polyvinylpyrrolidone (PVP) [161], pluronic 123 (P123) [162], tetrabutylammonium bromide [163], or biotemplates [164]. The use of templates could improve morphology, thermal stability, and the formation of active NiMoS/CoMoS phases [157]. Various morphologies as belt-like [158], fullerene-like [159], core-shell like [160] particles with more active sites were reported for unsupported HDS catalysts. The morphology and active phases depend on the content of the surfactant used in catalyst synthesis. Liu et al. [161] reported that  $\beta$ -NiMoO<sub>4</sub> phase is preferred in achieving highly active NiMoS phase with the high surface area can be obtained while low content of surfactant (PVP) used. Compared to supported catalysts, longer slab lengths are typically observed for the unsupported catalysts; this parameter seems to have more impact on the HDS activity than the stacking number [158,163]. A positive effect of carbon was observed for the catalyst synthesized using surfactant like cellulosic fibers [164] which is similar to the catalyst derived from the thermal decomposition of alkyl containing precursors (described in Section 3.2.1). Some of the experimental results confirmed that instead of an increase in stacking number, increase in slab length is more critical for high HDS selectivity [158,165]. As described in the previous sections, promoters increase the formation of the active phase. Indeed, the Cu promoted NbS<sub>2</sub> catalyst was more active than molybdenum sulfide per mass [162].

### 3.3. Concluding Remarks

Although unsupported catalysts are more active compared to supported catalysts, there are major drawbacks observed for these catalysts such as low surface area, sintering of the catalysts, etc. The unsupported catalysts derived from the thio-salts cannot be scaled up as the precursors are expensive and thus not economically viable. Furthermore, promoters oxidized when exposing to the

environment. Alternatively, synthesis of unsupported catalysts by precipitation and hydrothermal methods are eco-friendly. The catalysts activities can be further improved by an increase in surface area and in the dispersion which in turn depends on catalysts preparation method, precursors used, organic surfactants, etc. The degree of sulfidation, metal sulfide slab shape, size, length, and its orientation are the activity determining factors. Shorter slab lengths with a minimum of two slabs in a stack and larger Mo edges in the slabs are ideal to achieve hydrodesulfurization activity. Likewise, in supported catalysts, metal additives, promoter content, weak metal-sulfur bond energies, hydrogen as activation gas, moderate sulfidation temperatures (350–400 °C), etc. are also important for high HDS activity and selectivity of DDS/HYD route.

#### 4. Theoretical Studies

Theoretical studies, particularly those based on DFT calculations, have greatly contributed to the understanding of the physical/chemical properties of materials based on MoS<sub>2</sub> and their relationship with the experimentally observed properties. The theoretical results show that the bulk 2H-MoS<sub>2</sub> is a material that presents both direct and indirect band gaps with values very close to the experimentally reported [166–168], but also predict that the doping of this material with transition metals (or under pressure) could tailor their chemical, optical and electronic properties for the development of new interesting technological applications [169–171]. Also, a whole universe of possibilities arises with a reduction in dimensions of this kind of materials, which offers the possibilities of exploiting band-gap engineering [172–180] and of obtaining new magnetic properties [181–183].

Due to the important role that catalysts based on MoS<sub>2</sub> play in the petrochemical industry, theoretical studies have been focused on investigating the synergistic phenomena associated to the composition and distribution of the different atomic species, geometries, and support effects to improve the performance of catalysts in HDS processes. In that regard, theoretical results showed that for configurations that expose both bare Mo- and S-edges in the MoS<sub>2</sub> slabs, the metallic edges are preferential sites for catalysis whereas S-edges are inactive [184–187]. Consistently, recent studies [188] show that the main reaction route of thiophene HDS occurs along the CUS Mo-edge, whereas the activation of Mo-S connected edges is temperature dependent. On the other hand, Silva et al. [189] proposed an optimum cluster size suitable for catalysis studies, described as Mo<sub>27</sub>S<sub>x</sub>, which shows that different sulfur compounds could be adsorbed on several active sites of S- and Mo-edges [190]. Dynamic behavior of the 4,6-DMDBT molecule (switching between the  $\pi$  and  $\sigma$  adsorption) on brim and edge sites was observed by Gronborg et al. [191] through the DFT studies. It was shown that under HDS conditions formation of vacancy is unfavorable. Through scanning tunneling microscopy (STM) imaging the authors found that the (DDS route) adsorption of the 4,6-DMDBT molecule is possible only at the corner vacancy of the S-edge in the CoMoS nanocluster (Figure 8).

Although the doping or inclusion of transition metals like Fe, Co, Ni, Cu, Ru, W, or Pt, generally improve the performance of MoS<sub>2</sub> catalysts for numerous reactions [169,192–196], due to the particular interests in industrial processes, Ni and Co are the most studied dopants in the theoretical field.

Notably, the Ni as a promoter of the bimetallic catalyst (NiMoS), has the function of producing sulfur uncovered Lewis acid sites that favor HDS processes [197–199], resulting from the structural changes that modify the electronic properties of the surface. However, the incorporation of Ni on MoS<sub>2</sub> to form the NiMoS phase is not always more favorable than the formation of bulk nickel-sulfide compounds [200]. Similarly, when MoS<sub>2</sub> is promoted with Co (CoMoS), the barrier of hydrogenation reactions is reduced, and the C–S-scission reaction barrier increases [201–203] even when normally Co is known for favoring C–S bond scission much more than hydrogenation. Recent studies [204] reveal that smaller molecules like thiophene and methyl thiol prefer vacancies, while large molecules as 4,6-dimethyldibenzothiophene prefer physisorption on the brim of the edges or basal plane. The study of binding energy trends revealed that the nitrogen-containing compounds could strongly inhibit the HDS on the brim sites but have a minor effect on the CUS-like sites. In catalytic processes like

hydrodeoxygenation (HDO), the presence of oxygenated compounds (mainly water) may compromise the stability of the catalyst [205–208].

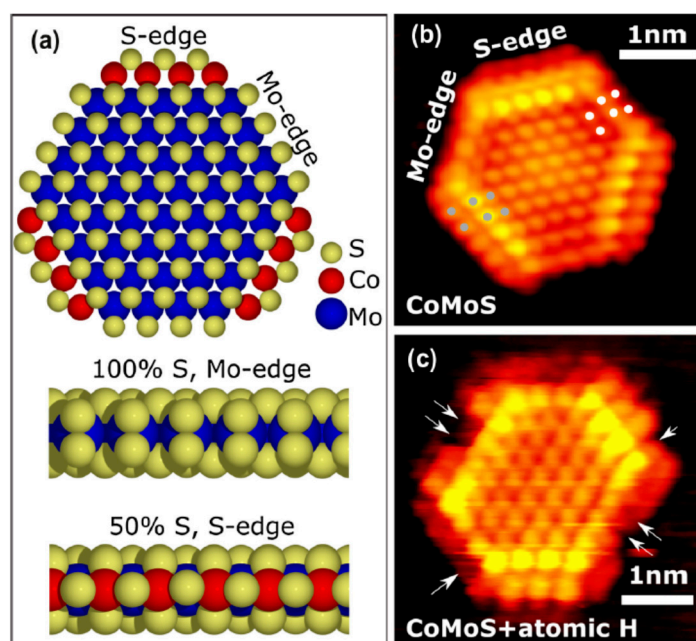


**Figure 8.** (a) Mo and S edges in CoMoS catalysts, (b) scanning tunneling microscopy (STM) images of the CoMoS nanocluster, (c) Formation of vacancies at the middle of Mo edge rather than the corner, on exposure of the hydrogen. Gronborg et al. [191].

Further studies show that, in comparison with non-promoted Mo catalysts, the CoMoS catalyst is more stable and is not deactivated due to the Co atoms that prevent sulfur–oxygen exchanges [209]. Also, under HDO conditions, the adsorption of guaiacol, phenol, and anisole was studied in the presence of compounds that can be present under reaction conditions ( $\text{H}_2\text{O}$ ,  $\text{H}_2\text{S}$ , and  $\text{CO}$ ), revealing the  $\eta^1$  adsorption mode leads to a direct deoxygenation reaction (DDO) and that  $\text{CO}$  is the major inhibitor in HDO process.

Studies of the possible configurations of trimetallic catalyst  $\text{Co}(\text{Ni})\text{Mo}$  compounds particularly under HDS conditions, showed that for periodic slab models under typical sulfidation conditions, Ni prefers to incorporate into the Mo-edge while Co prefers the S-edge [210]. Nevertheless, at the nanoscale and theoretically, the coexistence of Co–Mo or Ni–Mo edge is possible, although under HDS conditions the morphology adopted by the slabs is close to a hexagon where Co and Ni partially decorate the Me-edge, while the S-edge could partially be decorated by Ni [211]. Therefore, Ni or Co atoms participating in the promotion is a crucial parameter for optimizing the HDS/HYD selectivity ratio [212].

Although most of the catalytic reactions are directly related to the nature of the catalyst, the support may improve or reduce their catalytic properties, which is critical at the nanoscale, because the structure and the stability of the catalysts could be affected by the support [213,214]. One of the earliest theoretical efforts to understand the cluster/support interaction was motivated by the difference of catalytic activity presented by Type-I and Type-II CoMoS structures supported on alumina [215,216]. The results in these studies suggest that the weak interaction of Type-II CoMoS structures with the support may be due to the fact that in this case a highly endothermic process is required to create vacancies in such a way that the S linkages are severely reduced. Later on, Costa et al. [217] contrasted the effect of anatase- $\text{TiO}_2$  and  $\gamma\text{-Al}_2\text{O}_3$  supports on  $\text{MoS}_2$  and CoMoS catalysts, which showed that the higher HDS activity observed on anatase- $\text{TiO}_2$  is due to the strong edge-wetting and to the ligand effects that it presents. Recent studies confirm this effect with a more significant number of supports but considering a nanosized NiW catalyst [35]. Particularly in this last study, the interaction of a NiW catalyst with

two different SiO<sub>2</sub> supports presented different adsorption energies, as a consequence not only of the difference in sulfur-metal bond number but also because of the different morphological changes that the cluster suffered. This implies that the nature of the cluster/support interaction does not just depend on the composition of the support, but also on the metal-metal distances presented by the support at the surface.

### *Concluding Remarks*

Although the theoretical studies can help to unveil the nature of some of the mechanisms involved in the catalytic processes and to find newly improved catalysts, it is still not entirely clear the dependence on the catalytic properties imposed by different supports and their stability under different thermodynamic conditions. In this direction, these studies can help to develop new strategies to improve the catalyst performance (reaction stability) or to extend its lifetime.

## **5. General Conclusions**

The global tendency in ULSD fuels is to reduce the sulfur concentration to 10 ppm S or even lower to prevent air contamination in crowded cities. Zero sulfur emissions are a desirable goal in the mid-term for many advanced countries. These stringent requirements will need advanced HDS processes. However, due to the very high investment involved in the development of new processes, the more viable solution remains the advanced design of high-performance new-generation catalysts that can be adapted to the existent HDS units. These novel catalysts will have to eliminate complex sulfur molecules, preferentially by the direct desulfurization pathway reaction decreasing the consumption of hydrogen, to operate in the medium range of pressure (40–50 atm) with low space velocity values (1.5 h<sup>-1</sup> to 2.0 h<sup>-1</sup>) and must be ultra-stable.

The transition metal promoted catalysts widely used for decades remain very promising for the development of a new advanced generation of ULSD catalysts. However, they need to be tuned very precisely to obtain high-performance operation. Thus, for instance, the alumina support can be optimized by new additives or by the incorporation of second support with complementary surface properties with enormous possibilities to ameliorate the metal-support interaction, which could improve the morphology of the active phases and sites introducing better selectivities and with long-term stability.

For the catalytic removal of the sulfur from refractive compounds like DBT and its derivatives to achieve ULSD, the determining factors are typically active metal dispersion over support, metal-support interaction, active phases morphology, catalyst stability, among several others. In the case of supported catalysts, additives like P, B, F, Mg, Ga, and others could modify the metal support interactions and stability of the catalyst to achieve type-II active phases. For example, NiMoS or CoMoS type-II catalysts are less interactive with support and relatively highly active compared with type-I in the production of ultra-low sulfur fuels. Nevertheless, it is well known that in the metal sulfide catalysts based on Mo or W, the edges are those who presented higher activity. Therefore, dispersion factor regarding morphology, i.e., stacking number and slab lengths are necessary parameters to be improved for the deep removal of sulfur from refractive compounds such as DBT; methyl substituted DBT and others. Another critical factor that has to be considered is the use of chelating agents. Several recent research has pointed out that the use of a chelating agent could improve the dispersion of metals and also could increase the participation of promoter atoms in the nonstoichiometric phases CoMoS, NiMoS, or NiWS. The formation of complexes during the synthesis procedure also could delay the sulfidation of Co or Ni and therefore suppress the formation of bulk sulfides.

The use of unsupported catalysts derived from multi-metallic transition sulfides also offers excellent possibilities for improving the HDS catalytic properties for more demanding desulfurization conditions. Such catalysts offer a great variety of precursors with well-known chemical processes for the synthesis and the transformation to sulfides. Different morphologies are obtained, and different promoters/additives could be introduced to improve their activity or selectivity. For some precursors

such as the alkylthiometalates and under specific conditions (in situ, ex-situ, high pressure, among others), high surface areas (200–400 m<sup>2</sup>/g) with mesopore distribution could be obtained.

Finally, modeling methods by using advanced theoretical calculations will further continue to be excellent predictors to understand the catalytic properties of TMS by reproducing the experimental HDS results and electronic properties of experimental catalysts.

In conclusion, from the new experimental and theoretical reports about TMS catalysts performed in the last ten years, an optimistic future is open for developing new, better performing catalysts that will fulfill the societal needs for the near and far future.

**Author Contributions:** Writing-Review & Editing, J.N.D.d.L.; Writing-Original Draft Preparation, C.R.K. and J.A.-G.; Conceptualization and Supervision, S.F.-M.

**Funding:** Authors greatly thank the SENER-CONACyT-project 117373 for financial support.

**Acknowledgments:** Authors acknowledge the work of M. Isabel Perez Montfort who corrected the final version of this manuscript. Also, we want to thank the guest editor Anna Maria Venezia for inviting us to participate in this special issue.

**Conflicts of Interest:** The authors declare no conflict of interest.

## References

1. Refinery Catalysts Market, Global Trends and Forecasts to 2019 (Market Research Report), Markets and Markets. Available online: <https://www.marketsandmarkets.com> (accessed on 20 November 2018).
2. Speight, J.G.; Dekker, M. *The Desulfurization of Heavy Oils and Residua*, 2nd ed.; Marcel Dekker, Inc.: New York, NY, USA, 2000; ISBN 0-8247-8921-0.
3. Suresh, C.; Pérez-Cabrera, L.; Díaz de León, J.N.; Zepeda, T.A.; Alonso-Núñez, G.; Moyado, S.F. Highly active CoMo/Al(10) KIT-6 catalysts for HDS of DBT: Role of structure and aluminum heteroatom in the support matrix. *Catal. Today* **2017**, *296*, 214–218. [CrossRef]
4. Díaz de León, J.N.; Sánchez, L.A.; Toriello, Z.V.A.S.; Núñez, G.A.; Zepeda, T.A.; Yocupicio, R.I.; Reyes, J.A.L.; Fuentes, S. Support effects of NiW catalysts for highly selective sulfur removal from light hydrocarbons. *Appl. Catal. B Environ.* **2017**, *213*, 167–176. [CrossRef]
5. Stanislaus, A.; Marafi, A.; Rana, M.S. Recent advances in the science and technology of ultra low sulfur diesel (ULSD) production. *Catal. Today* **2010**, *153*, 1–68. [CrossRef]
6. International Maritime Organization [www.imo.org](http://www.imo.org). Available online: <http://www.imo.org/es/mediacentre/hottopics/paginas/sulphur-2020.aspx> (accessed on 7 January 2019).
7. Environmental Defense Fund Europe. Available online: <https://europe.edf.org/news/2018/31/07/alternative-fuels-future-zero-emissions-shipping> (accessed on 7 January 2019).
8. Hensen, E.J.M. *Hydrodesulfurization Catalysis and Mechanism of Supported Transition Metal Sulfides*; Eindhoven Technische Universiteit: Eindhoven, The Netherlands, 2000; ISBN 90-386-2871-4.
9. Topsoe, H.; Clausen, B.S.; Massoth, F.E. *Hydrotreating Catalysis Science and Technology*; Springer: Berlin/Hidelberg, Germany, 1996.
10. P.M.I. Comercio Internacional, S.A. de C.V. Available online: <http://www.pmi.com.mx> (accessed on 7 January 2019).
11. Mello, M.D.; Braggio, F.A.; Magalhães, B.C.; Zotin, J.L.; Silva, M.A.P. Kinetic modeling of deep hydrodesulfurization of dibenzothiophenes on NiMo/alumina catalysts modified by phosphorus. *Fuel Process. Technol.* **2018**, *177*, 66–74. [CrossRef]
12. Salazar, N.; Schmidt, S.B.; Lauritsen, J.V. Adsorption of nitrogenous inhibitor molecules on MoS<sub>2</sub> and CoMoS hydrodesulfurization catalysts particles investigated by scanning tunneling microscopy. *J. Catal.* **2019**, *370*, 232–240. [CrossRef]
13. Mallet, M.; Naboulsi, I.; Lebeau, B.; Aponte, C.F.L.; Brunet, S.; Michelin, L.; Bonne, M.; Carteret, C.; Blin, J.L. Selective direct desulfurization way (DDS) with CoMoS supported over mesostructured titania for the deep hydrodesulfurization of 4,6-dimethyldibenzothiophene. *Appl. Catal. A Gen.* **2018**, *563*, 91–97.
14. Macaud, M.; Milenkovic, A.; Schultz, E.; Lemaire, M.; Vrinat, M. Hydrodesulfurization of Alkyldibenzothiophenes: Evidence of Highly Unreactive Aromatic Sulfur Compounds. *J. Catal.* **2000**, *193*, 255–263. [CrossRef]

15. Rakotovao, V.R.; Diehl, F.; Brunet, S. Deep HDS of Diesel Fuel: Inhibiting Effect of Nitrogen Compounds on the Transformation of the Refractory 4,6-Dimethyldibenzothiophene Over a NiMoF/Al<sub>2</sub>O<sub>3</sub> Catalyst. *Catal. Lett.* **2009**, *129*, 50–60. [[CrossRef](#)]
16. Nie, H.; Li, H.; Yang, Q.; Li, D. Effect of structure and stability of active phase on catalytic performance of hydrotreating catalysts. *Catal. Today* **2018**, *316*, 13–20. [[CrossRef](#)]
17. Ibrahim, M.H.; Hayyan, M.; Hashim, M.A.; Hayyan, A. The role of ionic liquids in desulfurization of fuels: A review. *Renew. Sustain. Energy Rev.* **2017**, *76*, 1534–1549. [[CrossRef](#)]
18. Gatan, R.; Barger, P.; Gembicki, V.; Cavanna, A.; Molinari, D. Oxidative desulfurization: A new technology for ULSD. *Am. Chem. Soc. Div. Fuel Chem.* **2004**, *49*, 577–579.
19. Breyse, M.; Geantet, C.; Afanasiev, P.; Blanchard, J.; Vrinat, M. Recent studies on the preparation, activation and design of active phases and supports of hydrotreating catalysts. *Catal. Today* **2008**, *130*, 3–13. [[CrossRef](#)]
20. Besenbacher, F.; Brorson, M.; Clausen, B.S.; Helveg, S.; Hinnemann, B.; Kibsgaard, J.; Lauritsen, J.V.; Moses, P.G.; Nørskov, J.K.; Topsøe, H. Recent STM, DFT and HAADF-STEM studies of sulfide-based hydrotreating catalysts: Insight into mechanistic, structural and particle size effects. *Catal. Today* **2008**, *130*, 86–96. [[CrossRef](#)]
21. Chen, M.S.; Goodman, D.W. Structure–activity relationships in supported Au catalysts. *Catal. Today* **2006**, *111*, 22–33. [[CrossRef](#)]
22. Venezia, A.M.; Parola, V.L.; Liotta, L.F. Structural and surface properties of heterogeneous catalysts: Nature of the oxide carrier and supported particle size effects. *Catal. Today* **2017**, *285*, 114–124. [[CrossRef](#)]
23. Gutiérrez, O.Y.; Singh, S.; Schachtl, E.; Kim, J.; Kondratieva, E.; Hein, J.; Lercher, J.A. Effects of the Support on the Performance and Promotion of (Ni)MoS<sub>2</sub> Catalysts for Simultaneous Hydrodenitrogenation and Hydrodesulfurization. *ACS Catal.* **2014**, *4*, 1487–1499. [[CrossRef](#)]
24. Derouane, E.G.; Pedersen, E.; Clausen, B.S.; Gabelica, Z.; Candia, R.; Topsøe, H. EPR studies on unsupported and alumina-supported sulfided CoMo hydrodesulfurization catalysts. *J. Catal.* **1986**, *99*, 253–261. [[CrossRef](#)]
25. Topsøe, H. The role of Co–Mo–S type structures in hydrotreating catalysts. *Appl. Catal. A Gen.* **2007**, *322*, 3–8. [[CrossRef](#)]
26. Ninh, T.K.T.; Massin, L.; Laurenti, D.; Vrinat, M. A new approach in the evaluation of the support effect for NiMo hydrodesulfurization catalysts. *Appl. Catal. A Gen.* **2011**, *407*, 29–39. [[CrossRef](#)]
27. Shimada, H. Morphology and orientation of MoS<sub>2</sub> clusters on Al<sub>2</sub>O<sub>3</sub> and TiO<sub>2</sub> supports and their effect on catalytic performance. *Catal. Today* **2003**, *86*, 17–29. [[CrossRef](#)]
28. Bara, C.; Lamic-Humblot, A.F.; Fonda, E.; Gay, A.S.; Taleb, A.E.; Devers, E.; Digne, M.; Pirngruber, G.D.; Carrier, X. Surface-dependent sulfidation and orientation of MoS<sub>2</sub> slabs on alumina-supported model hydrodesulfurization catalysts. *J. Catal.* **2016**, *344*, 591–605. [[CrossRef](#)]
29. Sakashita, Y.; Araki, Y.; Honna, K.; Shimada, H. Orientation and morphology of molybdenum sulfide catalysts supported on titania particles, observed by using high-resolution electron microscopy. *Appl. Catal. A Gen.* **2000**, *197*, 247–253. [[CrossRef](#)]
30. Arrouvel, C.; Breyse, M.; Toulhoat, H.; Raybaud, P. A density functional theory comparison of anatase (TiO<sub>2</sub>)- and  $\gamma$ -Al<sub>2</sub>O<sub>3</sub>-supported MoS<sub>2</sub> catalysts. *J. Catal.* **2005**, *232*, 161–178. [[CrossRef](#)]
31. Díaz de León, J.N.; Zepeda, T.A.; Nuñez, G.A.; Galvan, D.H.; Pawelec, B.; Fuentes, S. Insight of 1D  $\gamma$ -Al<sub>2</sub>O<sub>3</sub> nanorods decoration by NiWS nanoslabs in ultra-deep hydrodesulfurization catalyst. *J. Catal.* **2015**, *321*, 51–61. [[CrossRef](#)]
32. Hayden, T.F.; Dumesic, J.A. Studies of the structure of molybdenum oxide and sulfide supported on thin films of alumina. *J. Catal.* **1987**, *103*, 366–384. [[CrossRef](#)]
33. Berhault, G. *New Materials for Catalytic Applications*; Elsevier: Amsterdam, The Netherlands, 2016; Volume 10, p. 336.
34. Nogueira, A.; Znaiguia, R.; Uzio, D.; Afanasiev, P.; Barhault, G. Curved nanostructures of unsupported and Al<sub>2</sub>O<sub>3</sub>-supported MoS<sub>2</sub> catalysts: Synthesis and HDS catalytic properties. *Appl. Catal. A Gen.* **2012**, *429–430*, 92–105. [[CrossRef](#)]
35. Díaz de León, J.N.; García, J.A.; Nuñez, G.A.; Zepeda, T.A.; Galvan, D.H.; de los Reyes, J.A.; Fuentes-Moyado, S. Support effects of NiW hydrodesulfurization catalysts from experiments and DFT calculations. *Appl. Catal. B Environ.* **2018**, *238*, 480–490. [[CrossRef](#)]
36. Iwata, Y.; Araki, Y.; Honna, K.; Miki, Y.; Sato, K.; Shimada, H. Hydrogenation active sites of unsupported molybdenum sulfide catalysts for hydroprocessing heavy oils. *Catal. Today* **2001**, *65*, 335–341. [[CrossRef](#)]

37. Afanasiev, P. Topotactic synthesis of size-tuned MoS<sub>2</sub> inorganic fullerenes that allows revealing particular catalytic properties of curved basal planes. *Appl. Catal. B Environ.* **2018**, *227*, 44–53. [[CrossRef](#)]
38. Laurenti, D.; Ngoc, B.P.; Massin, L.; Roukoss, C.; Devers, E.; Marchand, K.; Lemaitre, L.; Legens, C.; Quoineaud, A.A.; Vrinat, M. Intrinsic potential of alumina-supported CoMo catalysts in HDS: Comparison between  $\gamma$ C,  $\gamma$ T, and  $\delta$ -alumina. *J. Catal.* **2013**, *297*, 165–175. [[CrossRef](#)]
39. Araki, Y.; Honna, K.; Shimada, H. Formation and Catalytic Properties of Edge-Bonded Molybdenum Sulfide Catalysts on TiO<sub>2</sub>. *J. Catal.* **2002**, *207*, 361–370. [[CrossRef](#)]
40. Wang, H.; Wang, C.; Xiao, B.; Zhao, L.; Zhang, J.; Zhu, Y.; Guo, X. The hydroxyapatite nanotube as promoter to optimize the HDS reaction of NiMo/TiO<sub>2</sub> catalysts. *Catal. Today* **2016**, *259*, 340–346. [[CrossRef](#)]
41. Platanitis, P.; Panagiotou, G.D.; Bourikas, K.; Kordulis, C.; Fierro, J.L.G.; Lycourghiotis, A. Preparation of un-promoted molybdenum HDS catalysts supported on titania by equilibrium deposition filtration: Optimization of the preparative parameters and investigation of the promoting action of titania. *J. Mol. Catal. A Chem.* **2016**, *412*, 1–12. [[CrossRef](#)]
42. Villalón, P.C.; Ramírez, J.; Cuevas, R.; Vázquez, P.; Castañeda, R. Influence of the support on the catalytic performance of Mo, CoMo, and NiMo catalysts supported on Al<sub>2</sub>O<sub>3</sub> and TiO<sub>2</sub> during the HDS of thiophene, dibenzothiophene, or 4,6-dimethyldibenzothiophene. *Catal. Today* **2016**, *259*, 140–149. [[CrossRef](#)]
43. Mazurelle, J.; Lamonier, C.; Lancelot, C.; Payen, E.; Pichon, C.; Guillaume, D. Use of the cobalt salt of the heteropolyanion [Co<sub>2</sub>Mo<sub>10</sub>O<sub>38</sub>H<sub>4</sub>]<sup>6-</sup> for the preparation of CoMo HDS catalysts supported on Al<sub>2</sub>O<sub>3</sub>, TiO<sub>2</sub> and ZrO<sub>2</sub>. *Catal. Today* **2008**, *130*, 41–49. [[CrossRef](#)]
44. Laurenti, D.; Ninh, T.K.T.; Escalona, N.; Massin, L.; Vrinat, M.; Llambías, F.J.G. Support effect with rhenium sulfide catalysts. *Catal. Today* **2008**, *130*, 50–55. [[CrossRef](#)]
45. Ninh, T.K.T.; Laurenti, D.; Leclerc, E.; Vrinat, M. Support effect for CoMoS and CoNiMoS hydrodesulfurization catalysts prepared by controlled method. *Appl. Catal. A Gen.* **2014**, *487*, 210–218. [[CrossRef](#)]
46. Badoga, S.; Sharma, R.V.; Dalai, A.K.; Adjaye, J. Hydrotreating of heavy gas oil on mesoporous zirconia supported NiMo catalyst with EDTA. *Fuel* **2014**, *128*, 30–38. [[CrossRef](#)]
47. Baeza, P.; Aguila, G.; Gracia, F.; Araya, P. Desulfurization by adsorption with copper supported on zirconia. *Catal. Commun.* **2008**, *9*, 751–755. [[CrossRef](#)]
48. Song, S.; Zhou, X.; Duan, A.; Zhao, Z.; Chi, K.; Zhang, M.; Jiang, G.; Liu, J.; Li, J.; Wang, X. Synthesis of mesoporous silica material with ultra-large pore sizes and the HDS performance of dibenzothiophene. *Microporous Mesoporous Mater.* **2016**, *226*, 510–521. [[CrossRef](#)]
49. Parola, V.L.; Dragoi, B.; Ungureanu, A.; Dumitriu, E.; Venezia, A.M. New HDS catalysts based on thiol functionalized mesoporous silica supports. *Appl. Catal. A Gen.* **2010**, *386*, 43–50. [[CrossRef](#)]
50. Al-zaqri, N.; Alsalmeh, A.; Adil, S.F.; Alsaleh, A.; Alshammari, S.G.; Alresayes, S.I.; Alotaibi, R.; Al-Kinany, M.; Siddiqui, M.R.H. Comparative catalytic evaluation of nickel and cobalt substituted phosphomolybdic acid catalyst supported on silica for hydrodesulfurization of thiophene. *J. Saudi Chem. Soc.* **2017**, *21*, 965–973. [[CrossRef](#)]
51. Díaz de León, J.N. Binary  $\gamma$ -Al<sub>2</sub>O<sub>3</sub>- $\alpha$ -Ga<sub>2</sub>O<sub>3</sub> as supports of NiW catalysts for hydrocarbon sulfur removal. *Appl. Catal. B Environ.* **2016**, *181*, 524–533. [[CrossRef](#)]
52. Estrella, R.O.; Fierro, J.L.G.; Díaz de León, J.N.; Fuentes, S.; Nuñez, G.A.; Medina, E.L.; Pawelec, B.; Zepeda, T.A. Effect of partial Mo substitution by W on HDS activity using sulfide CoMoW/Al<sub>2</sub>O<sub>3</sub>-TiO<sub>2</sub> catalysts. *Fuel* **2018**, *233*, 644–657. [[CrossRef](#)]
53. Wan, G.; Duan, A.; Zhao, Z.; Jiang, G.; Zhang, D.; Li, R.; Dou, T.; Chung, K.H. Al<sub>2</sub>O<sub>3</sub>-TiO<sub>2</sub>/Al<sub>2</sub>O<sub>3</sub>-TiO<sub>2</sub>-SiO<sub>2</sub> Composite-Supported Bimetallic Pt-Pd Catalysts for the Hydrodearomatization and Hydrodesulfurization of Diesel Fuel. *Energy Fuels* **2009**, *23*, 81–85. [[CrossRef](#)]
54. Duan, A.; Li, R.; Jiang, G.; Gao, J.; Zhao, Z.; Wan, G.; Zhang, D.; Keng, W.H.; Chung, H. Hydrodesulfurization performance of NiW/TiO<sub>2</sub>-Al<sub>2</sub>O<sub>3</sub> catalyst for ultra clean diesel. *Catal. Today* **2009**, *140*, 187–191. [[CrossRef](#)]
55. Tavizon-Pozos, J.A.; Suarez-Toriello, V.A.; de los Reyes, J.A.; Lara, A.G.; Pawelec, B.; Fierro, J.L.G.; Vrinat, M.; Geantet, C. Deep Hydrodesulfurization of Dibenzothiophenes over NiW Sulfide Catalysts Supported on Sol-Gel Titania-Alumina. *Top. Catal.* **2016**, *59*, 241–251. [[CrossRef](#)]
56. Wang, H.; Yao, Z.; Zhan, X.; Wu, Y.; Li, M. Preparation of highly dispersed W/ZrO<sub>2</sub>-Al<sub>2</sub>O<sub>3</sub> hydrodesulfurization catalysts at high WO<sub>3</sub> loading via a microwave hydrothermal method. *Fuel* **2015**, *158*, 918–926. [[CrossRef](#)]

57. Vazquez-Garrido, I.; Benítez, A.L.; Berhault, G.; Guevara-Lara, A. Effect of support on the acidity of NiMo/Al<sub>2</sub>O<sub>3</sub>-MgO and NiMo/TiO<sub>2</sub>-Al<sub>2</sub>O<sub>3</sub> catalysts and on the resulting competitive hydrodesulfurization/hydrodenitrogenation reactions. *Fuel* **2019**, *236*, 55–64. [[CrossRef](#)]
58. Escobar, J.; Barrera, M.C.; Reyes, J.A.D.L.; Cortés, M.A.; Santes, V.; Gómez, E.; Pacheco, J.G. Effect of Mo and Co loading in HDS catalysts supported on solvo-thermally treated ZrO<sub>2</sub>-TiO<sub>2</sub> mixed oxides. *Catal. Today* **2008**, *133–135*, 282–291. [[CrossRef](#)]
59. Escobar, J.; De Los Reyes, J.A.; Ulín, C.A.; Barrera, M.C. Highly active sulfided CoMo catalysts supported on (ZrO<sub>2</sub>-TiO<sub>2</sub>)/Al<sub>2</sub>O<sub>3</sub> ternary oxides. *Mater. Chem. Phys.* **2013**, *143*, 213–222. [[CrossRef](#)]
60. Jabbarnezhad, P.; Haghighi, M.; Taghavinezhad, P. Sonochemical synthesis of NiMo/Al<sub>2</sub>O<sub>3</sub>-ZrO<sub>2</sub> nanocatalyst: Effect of sonication and zirconia loading on catalytic properties and performance in hydrodesulfurization reaction. *Fuel Process. Technol.* **2014**, *126*, 392–401. [[CrossRef](#)]
61. Daous, M.A.A.; Ali, S.A. Deep desulfurization of gas oil over NiMo catalysts supported on alumina-zirconia composites. *Fuel* **2012**, *97*, 662–669. [[CrossRef](#)]
62. Prado-Baston, E.; Boscaro-Franca, A.; da Silva Neto, A.V.; Urquieta-Gonzalez, E.A. Incorporation of the precursors of Mo and Ni oxides directly into the reaction mixture of sol-gel prepared  $\gamma$ -Al<sub>2</sub>O<sub>3</sub>-ZrO<sub>2</sub> supports – Evaluation of the sulfided catalysts in the thiophene hydrodesulfurization. *Catal. Today* **2015**, *246*, 184–190. [[CrossRef](#)]
63. Cruz-Pérez, A.E.; Jiménez, Y.T.; Alejo, J.J.V.; Zepeda, T.A.; Márquez, D.M.F.; Ruedas, M.G.R.; Fuentes-Moyado, S.; Díaz de León, J.N. NiW/MgO-TiO<sub>2</sub> catalysts for dibenzothiophene hydrodesulfurization: Effect of preparation method. *Catal. Today* **2016**, *271*, 28–34. [[CrossRef](#)]
64. Betancourt, J.C.M.; Benítez, A.L.; López, J.R.M.; Massin, L.; Aouine, M.; Vrinat, M.; Berhault, G.; Lara, A.G. Interaction effects of nickel polyoxotungstate with the Al<sub>2</sub>O<sub>3</sub>-MgO support for application in dibenzothiophene hydrodesulfurization. *J. Catal.* **2014**, *313*, 9–23. [[CrossRef](#)]
65. Benitez, A.L.; Berhault, G.; Lara, A.G. Addition of manganese to alumina and its influence on the formation of supported NiMo catalysts for dibenzothiophene hydrodesulfurization application. *J. Catal.* **2016**, *344*, 59–76. [[CrossRef](#)]
66. Benitez, A.L.; Berhault, G.; Burel, L.; Lara, A.G. Novel NiW hydrodesulfurization catalysts supported on Sol-Gel Mn-Al<sub>2</sub>O<sub>3</sub>. *J. Catal.* **2017**, *354*, 197–212. [[CrossRef](#)]
67. Benitez, A.L.; Berhault, G.; Lara, A.G. NiMo catalysts supported on Mn-Al<sub>2</sub>O<sub>3</sub> for dibenzothiophene hydrodesulfurization application. *Appl. Catal. B Environ.* **2017**, *213*, 28–41. [[CrossRef](#)]
68. Trejo, F.; Rana, M.M.S.; Ancheyta, J.; Chavez, S. Influence of support and supported phases on catalytic functionalities of hydrotreating catalysts. *Fuel* **2014**, *138*, 104–110. [[CrossRef](#)]
69. Nishijima, A.; Shimada, H.; Sato, T.; Yoshimura, Y.; Hiraishi, J. Support effects on hydrocracking and hydrogenation activities of molybdenum catalysts used for upgrading coal-derived liquids. *J. Polyhedron* **1986**, *5*, 243–247. [[CrossRef](#)]
70. Ramirez, J.; Rayo, P.; Alejandre, A.G.; Ancheyta, J.; Rana, M.S. Analysis of the hydrotreatment of Maya heavy crude with NiMo catalysts supported on TiO<sub>2</sub>-Al<sub>2</sub>O<sub>3</sub> binary oxides: Effect of the incorporation method of Ti. *Catal. Today* **2005**, *109*, 54–60. [[CrossRef](#)]
71. Maity, S.K.; Ancheyta, J.; Rana, M.S.; Rayo, P. Alumina-Titania Mixed Oxide Used as Support for Hydrotreating Catalysts of Maya Heavy Crude Effect of Support Preparation Methods. *Energy Fuels* **2006**, *20*, 427–431. [[CrossRef](#)]
72. Joshi, Y.V.; Ghosh, P.; Daage, M.; Delgass, W.N. Support effects in HDS catalysts: DFT analysis of thiolysis and hydrolysis energies of metal-support linkages. *J. Catal.* **2008**, *257*, 71–80. [[CrossRef](#)]
73. Zhu, Y.; Ramasse, Q.M.; Brorson, M.; Moses, P.G.; Hansen, L.P.; Kisielowski, C.F.; Helveg, S. Visualizing the stoichiometry of industrial-style Co-Mo-S catalysts with single-atom sensitivity. *Angew. Chem. Int. Ed.* **2014**, *53*, 10723–10727. [[CrossRef](#)]
74. Suarez-Toriello, V.A.; Vargas, C.E.S.; de los Reyes, J.A.; Zavala, A.V.; Vrinat, M.; Geantet, C. Influence of the solution pH in impregnation with citric acid and activity of Ni/W/Al<sub>2</sub>O<sub>3</sub> catalysts. *J. Mol. Catal. A Chem.* **2015**, *404–405*, 36–46. [[CrossRef](#)]
75. Wachs, I.E. *Characterization of Catalytic Materials*; Butterworth-Heinemann: Oxford, UK, 1992.
76. Díaz de León, J.N.; Picquart, M.; Villarroel, M.; Vrinat, M.; Llambias, F.J.G.; de los Reyes, J.A. Effect of gallium as an additive in hydrodesulfurization WS<sub>2</sub>/ $\gamma$ -Al<sub>2</sub>O<sub>3</sub> catalysts. *J. Mol. Catal. A Chem.* **2010**, *323*, 1–6. [[CrossRef](#)]

77. Hensen, E.J.M.; der Meer, Y.V.; Veen, J.A.R.V.; Niemantsverdriet, J.W. Insight into the formation of the active phases in supported NiW hydrotreating catalysts. *Appl. Catal. A Gen.* **2007**, *322*, 16–32. [[CrossRef](#)]
78. Coulier, L.; de Beer, V.H.J.; van Veen, J.A.R.; Niemantsverdriet, J.W. Correlation between Hydrodesulfurization Activity and Order of Ni and Mo Sulfidation in Planar Silica-Supported NiMo Catalysts: The Influence of Chelating Agents. *J. Catal.* **2001**, *197*, 26–33. [[CrossRef](#)]
79. Okamoto, Y.; Kato, A.; Usman; Sato, K.; Kubota, T. Co-WS<sub>2</sub> Hydrodesulfurization Catalysts: An Unexpected More Favorable Combination than Co-MoS<sub>2</sub>. *Chem. Lett.* **2005**, *34*, 1258–1259. [[CrossRef](#)]
80. Kubota, T.; Miyamoto, N.; Yoshioka, M.; Okamoto, Y. Surface structure and sulfidation behavior of Co-Mo and Co-W sulfide catalysts for the hydrodesulfurization of dibenzothiophene. *Appl. Catal. A Gen.* **2014**, *480*, 10–16. [[CrossRef](#)]
81. Vissenberg, M.J.; van der Meer, Y.; Hensen, E.J.M.; de Beer, V.H.J.; van der Kraan, A.M.; van Santen, R.A.; van Veen, J.A.R. The Effect of Support Interaction on the Sulfidability of Al<sub>2</sub>O<sub>3</sub>- and TiO<sub>2</sub>-Supported CoW and NiW Hydrodesulfurization Catalysts. *J. Catal.* **2001**, *198*, 151–163. [[CrossRef](#)]
82. Kishan, G.; Coulier, L.; van Veen, J.A.R.; Niemantsverdriet, J.W. Promoting Synergy in CoW Sulfide Hydrotreating Catalysts by Chelating Agents. *J. Catal.* **2001**, *200*, 194–196. [[CrossRef](#)]
83. Escobar, J.; Barrera, M.C.; Gutierrez, A.W.; Jacome, M.A.C.; Chavez, C.A.; Toledo, J.A.; Casados, D.A.S. Highly active P-doped sulfided NiMo/alumina HDS catalysts from Mo-blue by using saccharose as reducing agents precursor. *Appl. Catal. B Environ.* **2018**, *237*, 708–720. [[CrossRef](#)]
84. Mazoyer, P.; Geantet, C.; Diehl, F.; Loridant, S.; Lacroix, M. Role of chelating agent on the oxidic state of hydrotreating catalysts. *Catal. Today* **2008**, *130*, 75–79. [[CrossRef](#)]
85. de Jong, A.M.; de Beer, V.H.J.; Veen, J.A.R.; Niemantsverdriet, J.W. Surface Science Model of a Working Cobalt-Promoted Molybdenum Sulfide Hydrodesulfurization Catalyst: Characterization and Reactivity. *J. Phys. Chem.* **1996**, *100*, 17722–17724. [[CrossRef](#)]
86. Medici, L.; Prins, R. The Influence of Chelating Ligands on the Sulfidation of Ni and Mo in NiMo/SiO<sub>2</sub> Hydrotreating Catalysts. *J. Catal.* **1996**, *163*, 38–49. [[CrossRef](#)]
87. Van Haandel, L.; Bremmer, G.M.; Hensen, E.J.M.; Weber, T. The effect of organic additives and phosphoric acid on sulfidation and activity of (Co)Mo/Al<sub>2</sub>O<sub>3</sub> hydrodesulfurization catalysts. *J. Catal.* **2017**, *351*, 95–106. [[CrossRef](#)]
88. Blanchard, P.; Lamonier, C.; Griboval, A.; Payen, E. New insight in the preparation of alumina supported hydrotreatment oxidic precursors: A molecular approach. *Appl. Catal. A Gen.* **2007**, *322*, 33–45. [[CrossRef](#)]
89. Pashigreva, A.V.; Bukhtiyarova, G.A.; Klimov, O.V.; Chesalov, Y.A.; Litvak, G.S.; Noskov, A.S. Activity and sulfidation behavior of the CoMo/Al<sub>2</sub>O<sub>3</sub> hydrotreating catalyst: The effect of drying conditions. *Catal. Today* **2010**, *149*, 19–27. [[CrossRef](#)]
90. Wang, B.; Yu, W.; Meng, D.; Li, Z.; Xu, Y.; Ma, X. Effect of citric acid on CoO-MoO<sub>3</sub>/Al<sub>2</sub>O<sub>3</sub> catalysts for sulfur-resistant methanation. *React. Kinet. Mech. Catal.* **2018**, *125*, 111–126. [[CrossRef](#)]
91. Rinaldi, N.; Kubota, T.; Okamoto, Y. Effect of citric acid addition on the hydrodesulfurization activity of MoO<sub>3</sub>/Al<sub>2</sub>O<sub>3</sub> catalysts. *Appl. Catal. A Gen.* **2010**, *374*, 228–236. [[CrossRef](#)]
92. Magdaleno, M.A.C.; Nieto, J.A.M.; Klimova, T.E. Effect of the amount of citric acid used in the preparation of NiMo/SBA-15 catalysts on their performance in HDS of dibenzothiophene-type compounds. *Catal. Today* **2014**, *220–222*, 78–88. [[CrossRef](#)]
93. Wu, H.; Duan, A.; Zhao, Z.; Qi, D.; Li, J.; Liu, B.; Jiang, G.; Liu, J.; Wei, Y.; Zhang, X. Preparation of NiMo/KIT-6 hydrodesulfurization catalysts with tunable sulfidation and dispersion degrees of active phase by addition of citric acid as chelating agent. *Fuel* **2014**, *130*, 203–210. [[CrossRef](#)]
94. Chen, J.; Maugé, F.; Fallah, J.E.; Oliviero, L. IR spectroscopy evidence of MoS<sub>2</sub> morphology change by citric acid addition on MoS<sub>2</sub>/Al<sub>2</sub>O<sub>3</sub> catalysts—A step forward to differentiate the reactivity of M-edge and S-edge. *J. Catal.* **2014**, *320*, 170–179. [[CrossRef](#)]
95. Nikulshin, P.A.; Ishutenko, D.I.; Mozhaev, A.A.; Maslakov, K.I.; Pimerzin, A.A. Effects of composition and morphology of active phase of CoMo/Al<sub>2</sub>O<sub>3</sub> catalysts prepared using Co<sub>2</sub>Mo<sub>10</sub>-heteropolyacid and chelating agents on their catalytic properties in HDS and HYD reactions. *J. Catal.* **2014**, *312*, 152–169. [[CrossRef](#)]
96. Rinaldi, N.; Kubota, T.; Okamoto, Y. Effect of Citric Acid Addition on Co-Mo/B<sub>2</sub>O<sub>3</sub>/Al<sub>2</sub>O<sub>3</sub> Catalysts Prepared by a Post-Treatment Method. *Ind. Eng. Chem. Res.* **2009**, *48*, 10414–10424. [[CrossRef](#)]
97. Li, H.; Li, M.; Chu, Y.; Liu, F.; Nie, H. Essential role of citric acid in preparation of efficient NiW/Al<sub>2</sub>O<sub>3</sub> HDS catalysts. *Appl. Catal. A Gen.* **2011**, *403*, 75–82. [[CrossRef](#)]

98. Valencia, D.; Klimova, T. Kinetic study of NiMo/SBA-15 catalysts prepared with citric acid in hydrodesulfurization of dibenzothiophene. *Catal. Commun.* **2012**, *21*, 77–81. [[CrossRef](#)]
99. Valencia, D.; Klimova, T. Citric acid loading for MoS<sub>2</sub>-based catalysts supported on SBA-15. New catalytic materials with high hydrogenolysis ability in hydrodesulfurization. *Appl. Catal. B Environ.* **2013**, *129*, 137–145. [[CrossRef](#)]
100. Klimova, T.E.; Valencia, D.; Nieto, J.A.M.; Hipólito, P.H. Behavior of NiMo/SBA-15 catalysts prepared with citric acid in simultaneous hydrodesulfurization of dibenzothiophene and 4,6-dimethyldibenzothiophene. *J. Catal.* **2013**, *304*, 29–46. [[CrossRef](#)]
101. Villalón, P.C.; Ramirez, J.; Luciano, J.V. Analysis of the role of citric acid in the preparation of highly active HDS catalysts. *J. Catal.* **2014**, *320*, 127–136. [[CrossRef](#)]
102. Dufresne, P. Hydroprocessing catalysts regeneration and recycling. *Appl. Catal. A Gen.* **2007**, *322*, 67–75. [[CrossRef](#)]
103. Bui, N.Q.; Geantet, C.; Berhault, G. Maleic acid, an efficient additive for the activation of regenerated CoMo/Al<sub>2</sub>O<sub>3</sub> hydrotreating catalysts. *J. Catal.* **2015**, *330*, 374–386. [[CrossRef](#)]
104. Pimerzin, A.; Roganov, A.; Mozhaev, A.; Maslakov, K.; Nikulshin, P.; Pimerzin, A. Active phase transformation in industrial CoMo/Al<sub>2</sub>O<sub>3</sub> hydrotreating catalyst during its deactivation and rejuvenation with organic chemicals treatment. *Fuel Process. Technol.* **2018**, *173*, 56–65.
105. Zhang, Y.; Han, W.; Long, X.; Nie, H. Redispersion effects of citric acid on CoMo/γ-Al<sub>2</sub>O<sub>3</sub> hydrodesulfurization catalysts. *Catal. Commun.* **2016**, *82*, 20–23. [[CrossRef](#)]
106. Han, W.; Nie, H.; Long, X.; Li, M.; Yang, Q.; Li, D. Preparation of F-doped MoS<sub>2</sub>/Al<sub>2</sub>O<sub>3</sub> catalysts as a way to understand the electronic effects of the support Brønsted acidity on HDN activity. *J. Catal.* **2016**, *339*, 135–142. [[CrossRef](#)]
107. Han, W.; Nie, H.; Long, X.; Li, M.; Yang, Q.; Li, D. Effects of the support Brønsted acidity on the hydrodesulfurization and hydrodenitrogenation activity of sulfided NiMo/Al<sub>2</sub>O<sub>3</sub> catalysts. *Catal. Today* **2017**, *292*, 58–66. [[CrossRef](#)]
108. Caloch, B.; Rana, M.S.; Ancheyta, J. Improved hydrogenolysis (C–S, C–M) function with basic supported hydrodesulfurization catalysts. *Catal. Today* **2004**, *98*, 91–98. [[CrossRef](#)]
109. Kumar, M.; Aberuagba, F.; Gupta, J.K.; Rawat, K.S.; Sharma, L.D.; Murali Dhar, G. Temperature-programmed reduction and acidic properties of molybdenum supported on MgO–Al<sub>2</sub>O<sub>3</sub> and their correlation with catalytic activity. *J. Mol. Catal. A Chem.* **2004**, *213*, 217–223. [[CrossRef](#)]
110. Trejo, F.; Rana, M.S.; Ancheyta, J. CoMo/MgO–Al<sub>2</sub>O<sub>3</sub> supported catalysts: An alternative approach to prepare HDS catalysts. *Catal. Today* **2008**, *130*, 327–336. [[CrossRef](#)]
111. Chen, W.; Nie, H.; Li, D.; Long, X.; van Gestel, J.; Maugé, F. Effect of Mg addition on the structure and performance of sulfide Mo/Al<sub>2</sub>O<sub>3</sub> in HDS and HDN reaction. *J. Catal.* **2016**, *344*, 420–433. [[CrossRef](#)]
112. Rashidi, F.; Sasaki, T.; Rashidi, A.M.; Kharat, A.N.; Jozani, K.J. Ultradeep hydrodesulfurization of diesel fuels using highly efficient nanoalumina-supported catalysts: Impact of support, phosphorus, and/or boron on the structure and catalytic activity. *J. Catal.* **2013**, *299*, 321–335. [[CrossRef](#)]
113. Klimov, O.V.; Vatutina, Y.V.; Nadeina, K.A.; Kazakov, M.O.; Gerasimov, E.Y.; Prosvirin, I.P.; Larina, T.V.; Noskov, A.S. CoMoB/Al<sub>2</sub>O<sub>3</sub> catalysts for hydrotreating of diesel fuel. The effect of the way of the boron addition to a support or an impregnating solution. *Catal. Today* **2018**, *305*, 192–202. [[CrossRef](#)]
114. Vatutina, Y.V.; Klimov, O.V.; Nadeina, K.A.; Danilova, I.G.; Gerasimov, E.Y.; Prosvirin, I.P.; Noskov, A.S. Influence of boron addition to alumina support by kneading on morphology and activity of HDS catalysts. *Appl. Catal. B Environ.* **2016**, *199*, 23–32. [[CrossRef](#)]
115. Usman; Kubota, T.; Hiromitsu, I.; Okamoto, Y. Effect of boron addition on the surface structure of Co–Mo/Al<sub>2</sub>O<sub>3</sub> catalysts. *J. Catal.* **2007**, *247*, 78–85. [[CrossRef](#)]
116. Chen, W.; Maugé, F.; Van Gestel, J.; Nie, H.; Li, D.; Long, X. Effect of modification of the alumina acidity on the properties of supported Mo and CoMo sulfide catalysts. *J. Catal.* **2013**, *304*, 47–62. [[CrossRef](#)]
117. Klimov, O.V.; Nadeina, K.A.; Vatutina, Y.V.; Stolyarova, E.A.; Danilova, I.G.; Gerasimov, E.Y.; Prosvirin, I.P.; Noskov, A.S. CoMo/Al<sub>2</sub>O<sub>3</sub> hydrotreating catalysts of diesel fuel with improved hydrodenitrogenation activity. *Catal. Today* **2018**, *307*, 73–83. [[CrossRef](#)]
118. Tong, R.L.; Wang, Y.G.; Zhang, X.; Zhang, H.Y.; Dai, J.Z.; Lin, X.C.; Xu, D.P. Effect of phosphorus modification on the catalytic properties of NiW/γ-Al<sub>2</sub>O<sub>3</sub> in the hydrogenation of aromatics from coal tar. *J. Fuel Chem. Technol.* **2015**, *43*, 1461–1469. [[CrossRef](#)]

119. García-Vila, A.; Cuevas-García, R.; Ramírez, J.; Puente-Lee, I. Effect of phosphorus on Mo/Al<sub>2</sub>O<sub>3</sub> catalysts for Maya crude improvement. *Catal. Today* **2014**, *220–222*, 310–317. [[CrossRef](#)]
120. Altamirano, E.; de Los Reyes, J.A.; Murrieta, F.; Vrinat, M. Hydrodesulfurization of dibenzothiophene and 4,6-dimethyl-dibenzothiophene: Gallium effect over NiMo/Al<sub>2</sub>O<sub>3</sub> sulfided catalysts. *J. Catal.* **2005**, *235*, 403–412. [[CrossRef](#)]
121. Altamirano, E.; de Los Reyes, J.A.; Murrieta, F.; Vrinat, M. Hydrodesulfurization of 4,6-dimethyldibenzothiophene over Co(Ni)MoS<sub>2</sub> catalysts supported on alumina: Effect of gallium as an additive. *Catal. Today* **2008**, *133–135*, 292–298. [[CrossRef](#)]
122. Díaz de León, J.N.; Picquart, M.; Massin, L.; Vrinat, M.; de los Reyes, J.A. Hydrodesulfurization of sulfur refractory compounds: Effect of gallium as an additive in NiWS/γ-Al<sub>2</sub>O<sub>3</sub> catalysts. *J. Mol. Catal. A Chem.* **2012**, *363–364*, 311–321. [[CrossRef](#)]
123. Zhou, W.; Zhang, Y.; Tao, X.; Zhou, Y.; Wei, Q.; Ding, S. Effects of gallium addition to mesoporous alumina by impregnation on dibenzothiophene hydrodesulfurization performances of the corresponding NiMo supported catalysts. *Fuel* **2018**, *228*, 152–163. [[CrossRef](#)]
124. Olivas, A.; Luque, P.A.; Gómez-Gutierrez, C.M.; Flores, D.L.; Valdez, R.; Escalante, L.; Schacht, P.; Silva-Rodrigo, R. Synthesis and characterization of mesoporous supports doped with NiW/Gax for hydrodesulfurization of DBT. *Catal. Comm.* **2017**, *91*, 67–71. [[CrossRef](#)]
125. Zhou, W.; Zhang, Q.; Zhou, Y.; Wei, Q.; Du, L.; Ding, S.; Jiang, S.; Zhang, Y. Effects of Ga- and P-modified USY-based NiMoS catalysts on ultra-deep hydrodesulfurization for FCC diesels. *Catal. Today* **2018**, *305*, 171–181. [[CrossRef](#)]
126. Reinhoudt, H.R.; Crezee, E.; van Langeveld, A.D.; Kooyman, P.J.; Moulijn, J.A. Characterization of the Active Phase in NiW/γ-Al<sub>2</sub>O<sub>3</sub> Catalysts in Various Stages of Sulfidation with FTIR(NO) and XPS. *J. Catal.* **2000**, *196*, 315–329. [[CrossRef](#)]
127. Moses, P.G.; Hinnemann, B.; Topsoe, H.; Norskov, J.K. The hydrogenation and direct desulfurization reaction pathway in thiophene hydrodesulfurization over MoS<sub>2</sub> catalysts at realistic conditions: A density functional study. *J. Catal.* **2007**, *248*, 188–203. [[CrossRef](#)]
128. Yoosuk, B.; Song, C.; Kim, J.H.; Ngamcharussrivichai, C.; Prasassarakich, P. Effects of preparation conditions in hydrothermal synthesis of highly active unsupported NiMo sulfide catalysts for simultaneous hydrodesulfurization of dibenzothiophene and 4,6-dimethyldibenzothiophene. *Catal. Today* **2010**, *149*, 52–61. [[CrossRef](#)]
129. Fontaine, C.; Romero, Y.; Daudin, A.; Devers, E.; Bouchy, C.; Brunet, S. Insight into sulphur compounds and promoter effects on Molybdenum-based catalysts for selective HDS of FCC gasoline. *Appl. Catal. A Gen.* **2010**, *388*, 188–195. [[CrossRef](#)]
130. Niefind, F.; Bensch, W.; Deng, M.; Kienle, L.; Reyes, J.C.; Granados, J.M.D.V. Co-promoted MoS<sub>2</sub> for hydrodesulfurization: New preparation method of MoS<sub>2</sub> at room temperature and observation of massive differences of the selectivity depending on the activation atmosphere. *Appl. Catal. A Gen.* **2015**, *497*, 72–84. [[CrossRef](#)]
131. Zhang, B.S.; Yi, Y.J.; Zhang, W.; Liang, C.H.; Su, D.S. Electron microscopy investigation of the microstructure of unsupported Ni–Mo–W sulfide. *Mater. Charact.* **2011**, *62*, 684–690. [[CrossRef](#)]
132. Acuña, R.H.; Nunez, G.A.; Delgado, F.P.; Romero, J.L.; Berhault, G.; Munoz, E.M.R. Unsupported trimetallic CoMoW sulfide HDS catalysts prepared by in situ decomposition of sulfur-containing precursors. *Catal. Today* **2015**, *250*, 28–37. [[CrossRef](#)]
133. Armenta, Y.E.; Reyes, J.C.; Delgado, F.P.; Valle, M.D.; Alonso, G.; Fuentes, S.; Rivera, R.R. CoMoW sulfide nanocatalysts for the HDS of DBT from novel ammonium and alkyltrimethylammonium-thiomolybdate-thiotungstate-cobaltate (II) precursors. *Appl. Catal. A Gen.* **2014**, *486*, 62–68. [[CrossRef](#)]
134. Romero, L.; Valle, M.D.; Rivera, R.R.; Alonso, G.; Borja, M.A.; Fuentes, S.; Delgado, F.P.; Reyesa, J.C. MoS<sub>2</sub> catalysts derived from n-methylenediammonium thiomolybdates during HDS of DBT. *Catal. Today* **2015**, *250*, 66–71. [[CrossRef](#)]
135. Le, Z.; Afanasiev, P.; Li, D.; Shi, Y.; Vrinat, M. Synthesis of unsupported Ni–W–S hydrotreating catalysts from the oxothiosalt (NH<sub>4</sub>)<sub>2</sub>WO<sub>2</sub>S<sub>2</sub>. *C. R. Chim.* **2008**, *11*, 130–136. [[CrossRef](#)]
136. Hur, Y.G.; Lee, D.W.; Lee, K.Y. Hydrocracking of vacuum residue using NiWS(x) dispersed catalysts. *Fuel* **2016**, *185*, 794–803. [[CrossRef](#)]

137. Ho, T.C.; McConnachie, J.M. Ultra-deep hydrodesulfurization on MoS<sub>2</sub> and Co<sub>0.1</sub>MoS<sub>2</sub>: Intrinsic vs. environmental factors. *J. Catal.* **2011**, *277*, 117–122. [[CrossRef](#)]
138. Olivas, A.; Zepeda, T.A.; Villalpando, I.; Fuentes, S. Performance of unsupported Ni(Co,Fe)/MoS<sub>2</sub> catalysts in hydrotreating reactions. *Catal. Commun.* **2008**, *9*, 1317–1328. [[CrossRef](#)]
139. Yi, Y.; Zhang, B.; Jin, X.; Wang, L.; Williams, C.T.; Xiong, G.; Su, D.; Liang, C. Unsupported NiMoW sulfide catalysts for hydrodesulfurization of dibenzothiophene by thermal decomposition of thiosalts. *J. Mol. Catal. A Chem.* **2011**, *351*, 120–127. [[CrossRef](#)]
140. Bocarando, J.; Acuna, R.H.; Bensch, W.; Huang, Z.D.; Petranovskii, V.; Fuentes, S.; Nunez, G.A. Unsupported Ni-Mo-W sulphide HDS catalysts with the varying nickel concentration. *Appl. Catal. A Gen.* **2009**, *363*, 45–51. [[CrossRef](#)]
141. Zepeda, T.A.; Pawelec, B.; Díaz de León, J.N.; de los Reyes, J.A.; Olivas, A. Effect of gallium loading on the hydrodesulfurization activity of unsupported Ga<sub>2</sub>S<sub>3</sub>/WS<sub>2</sub> catalysts. *Appl. Catal. B Environ.* **2012**, *111–112*, 10–19. [[CrossRef](#)]
142. Daudin, A.; Lamic, A.F.; Perot, G.; Brunet, S.; Raybaud, P.; Bouchy, C. Microkinetic interpretation of HDS/HYDO selectivity of the transformation of a model FCC gasoline over transition metal sulfides. *Catal. Today* **2008**, *130*, 221–230. [[CrossRef](#)]
143. Afanasiev, P. The influence of reducing and sulfiding conditions on the properties of unsupported MoS<sub>2</sub>-based catalysts. *J. Catal.* **2010**, *269*, 269–280. [[CrossRef](#)]
144. Amaya, S.L.; Nunez, G.A.; Zepeda, T.A.; Fuentes, S.; Echavarria, A. Effect of the divalent metal and the activation temperature of NiMoW and CoMoW on the dibenzothiophene hydrodesulfurization reaction. *Appl. Catal. B Environ.* **2014**, *148–149*, 221–230. [[CrossRef](#)]
145. Coelho, T.L.; Licea, Y.E.; Palacio, L.A.; Faro, A.C., Jr. Heptamolybdate-intercalated CoMgAl hydrotalcites as precursors for HDS-selective hydrotreating catalysts. *Catal. Today* **2015**, *250*, 38–46. [[CrossRef](#)]
146. Amaya, S.L.; Nunez, G.A.; Reyes, J.C.; Fuentes, S.; Echavarria, A. Influence of the sulfidation temperature in a NiMoW catalyst derived from layered structure (NH<sub>4</sub>)Ni<sub>2</sub>OH(H<sub>2</sub>O)(MoO<sub>4</sub>)<sub>2</sub>. *Fuel* **2015**, *139*, 575–583. [[CrossRef](#)]
147. Chen, Y.; Wang, L.; Zhang, Y.; Liu, T.; Liu, X.; Jiang, Z.; Li, C. A new multi-metallic bulk catalyst with high hydrodesulfurization activity of 4,6-DMDBT prepared using layered hydroxide salts as structural templates. *Appl. Catal. A Gen.* **2014**, *474*, 69–77. [[CrossRef](#)]
148. Yin, C.; Wang, Y.; Xue, S.; Liu, H.; Li, H.; Liu, C. Influence of sulfidation conditions on morphology and hydrotreating performance of unsupported Ni–Mo–W catalysts. *Fuel* **2016**, *175*, 13–19. [[CrossRef](#)]
149. Zhang, H.; Lin, H.; Zheng, Y.; Hu, Y.; MacLennan, A. Understanding of the effect of synthesis temperature on the crystallization and activity of nano-MoS<sub>2</sub> catalyst. *Appl. Catal. B Environ.* **2015**, *165*, 537–546. [[CrossRef](#)]
150. Long, Y.C.; Ping, Z.X.; Yyan, Z.L.; Guang, L.C. Mechanism of Hydrodesulfurization of dibenzothiophenes on unsupported NiMoW catalyst. *J. Fuel Chem. Technol.* **2013**, *41*, 991–997.
151. Liu, C.; Liu, H.; Yin, C.; Zhao, X.; Liu, B.; Li, X.; Li, Y.; Liu, Y. Preparation, characterization, and hydrodesulfurization properties of binary transition-metal sulfide catalysts. *Fuel* **2015**, *154*, 88–94. [[CrossRef](#)]
152. Liu, H.; Liu, C.; Yin, C.; Chai, Y.; Li, Y.; Liu, D.; Liu, B.; Li, X.; Wang, Y.; Li, X. Preparation of highly active unsupported nickel–zinc–molybdenum catalysts for the hydrodesulfurization of dibenzothiophene. *Appl. Catal. B Environ.* **2015**, *174–175*, 264–276. [[CrossRef](#)]
153. Liu, H.; Yin, C.; Li, H.; Liu, B.; Li, X.; Chai, Y.; Li, Y.; Liu, C. Synthesis, characterization and hydrodesulfurization properties of nickel–copper–molybdenum catalysts for the production of ultra-low sulfur diesel. *Fuel* **2014**, *129*, 138–146. [[CrossRef](#)]
154. Yue, L.; Li, G.; Zhang, F.; Chen, L.; Li, X.; Huang, X. Size-dependent activity of unsupported Co–Mo sulfide catalysts for the hydrodesulfurization of dibenzothiophene. *Appl. Catal. A Gen.* **2016**, *512*, 85–92. [[CrossRef](#)]
155. Theodet, M.; Quilfen, C.; Martinez, C.; Aymonier, C. Continuous supercritical synthesis of unsupported and high specific surface area catalyst precursors for deep-hydrodesulfurization. *J. Supercrit. Fluids* **2016**, *117*, 252–259. [[CrossRef](#)]
156. Farag, H.; Kishida, M.; Megren, H.A. Competitive hydrodesulfurization of dibenzothiophene and hydrodenitrogenation of quinoline over unsupported MoS<sub>2</sub> catalyst. *Appl. Catal. A Gen.* **2014**, *469*, 173–182. [[CrossRef](#)]
157. Yin, C.; Zhao, L.; Bai, Z.; Liu, H.; Liu, Y.; Liu, C. A novel porous ammonium nickel molybdate as the catalyst precursor towards deep hydrodesulfurization of gas oil. *Fuel* **2013**, *107*, 873–878. [[CrossRef](#)]

158. Li, P.; Chen, Y.; Zhang, C.; Huang, B.; Liu, X.; Liu, T.; Jiang, Z.; Li, C. Highly selective hydrodesulfurization of gasoline on unsupported Co-Mo sulfide catalysts: Effect of MoS<sub>2</sub> morphology. *Appl. Catal. A Gen.* **2017**, *533*, 99–108. [[CrossRef](#)]
159. Blanco, E.; Uzio, D.; Berhault, G.; Afanasiev, P. From core-shell MoS<sub>x</sub>/ZnS to open fullerene-like MoS<sub>2</sub> nanoparticles. *J. Mater. Chem. A* **2014**, *2*, 3325–3331. [[CrossRef](#)]
160. Aissa, A.H.; Dassenoy, F.; Geantet, C.; Afanasiev, P. Solution synthesis of core-shell Co<sub>9</sub>S<sub>8</sub>@MoS<sub>2</sub> catalysts. *Catal. Sci. Technol.* **2016**, *6*, 4901–4909. [[CrossRef](#)]
161. Liu, H.; Yin, C.; Li, X.; Chai, Y.; Li, Y.; Liu, C. Effect of NiMo phases on the hydrodesulfurization activities of dibenzothiophene. *Catal. Today* **2017**, *282*, 222–229. [[CrossRef](#)]
162. Mansouri, A.; Semagina, N. Promotion of Niobium Oxide Sulfidation by Copper and Its Effects on Hydrodesulfurization Catalysis. *ACS Catal.* **2018**, *8*, 7621–7632. [[CrossRef](#)]
163. Le, Z.; Xiangyun, L.; Dadong, L.; Xiaodong, G. Study on high-performance unsupported Ni-Mo-W hydrotreating catalyst. *Catal. Commun.* **2011**, *12*, 927–931.
164. Afanasiev, P.; Geantet, C.; Llorens, I.; Proux, O. Biotemplated synthesis of highly divided MoS<sub>2</sub> catalysts. *J. Mater. Chem.* **2012**, *22*, 9731–9737. [[CrossRef](#)]
165. Zhang, C.; Li, P.; Liu, X.; Liu, T.; Jiang, Z.; Li, C. Morphology-performance relation of (Co)MoS<sub>2</sub> catalysts in the hydrodesulfurization of FCC gasoline. *Appl. Catal. A Gen.* **2018**, *556*, 20–28. [[CrossRef](#)]
166. Gusakova, J.; Wang, X.; Lynn Shiau, L.; Krivosheeva, A.; Shaposhnikov, V.; Borisenko, V.; Gusakov, V.; Kang Tay, B. Electronic Properties of Bulk and Monolayer TMDs: Theoretical Study Within DFT Framework (GVJ-2e Method). *Phys. Status Solidi A* **2017**, *214*, 1700218. [[CrossRef](#)]
167. Coutinho, S.S.; Tavares, M.S.; Barboza, C.A.; Frazão, N.F.; Moreira, E.; Azevedo, D.L. 3R and 2H polytypes of MoS<sub>2</sub>: DFT and DFPT calculations of structural, optoelectronic, vibrational and thermodynamic properties. *J. Phys. Chem. Solids* **2017**, *111*, 25–33. [[CrossRef](#)]
168. Ivanovskaya, V.V.; Zobelli, A.; Gloter, A.; Brun, N.; Serin, V.; Colliex, C. Ab initio study of bilateral doping within the MoS<sub>2</sub>-NbS<sub>2</sub> system. *Phys. Rev. B* **2008**, *78*, 134104. [[CrossRef](#)]
169. Olivas, A.; Antúnez-García, J.; Fuentes, S.; Galván, D.H. Electronic properties of unsupported trimetallic catalysts. *Catal. Today* **2014**, *220–222*, 106–112. [[CrossRef](#)]
170. Suh, J.; Leong Tan, T.; Zhao, W.; Park, J.; Lin, D.-Y.; Park, T.-E.; Kim, J.; Jin, C.; Saigal, N.; Ghosh, S.; et al. Reconfiguring crystal and electronic structures of MoS<sub>2</sub> by substitutional doping. *Nat. Commun.* **2018**, *9*, 199. [[CrossRef](#)] [[PubMed](#)]
171. Brotons-Gisbert, M.; Segura, A.; Robles, R.; Canadell, E.; Ordejón, P.; Sánchez-Royo, J.F. Optical and electronic properties of 2H-MoS<sub>2</sub> under pressure: Revealing the spin-polarized nature of bulk electronic bands. *Phys. Rev. Mater.* **2018**, *2*, 054602. [[CrossRef](#)]
172. Zhou, W.; Zou, X.; Najmaei, S.; Liu, Z.; Shi, Y.; Kong, J.; Lou, J.; Ajayan, P.M.; Yakobson, B.I.; Idrobo, J.-C. Intrinsic Structural Defects in Monolayer Molybdenum Disulfide. *Nano Lett.* **2013**, *13*, 2615–2622. [[CrossRef](#)] [[PubMed](#)]
173. Wan, H.; Xu, L.; Huang, W.Q.; Zhou, J.H.; He, C.N.; Li, X.; Huang, G.F.; Peng, P.; Zhou, Z.G. Band structure engineering of monolayer MoS<sub>2</sub>: A charge compensated codoping strategy. *RSC Adv.* **2015**, *5*, 7944–7952. [[CrossRef](#)]
174. Tang, Q.; Jiang, D.E. Stabilization and band-gap tuning of the 1T-MoS<sub>2</sub> monolayer by covalent functionalization. *Chem. Mater.* **2015**, *27*, 3743–3748. [[CrossRef](#)]
175. Krivosheeva, A.V.; Shaposhnikov, V.L.; Borisenko, V.E.; Lazzari, J.L.; Waileong, C.; Gusakova, J.; Tay, B.K. Theoretical study of defect impact on two-dimensional MoS<sub>2</sub>. *J. Semicond.* **2015**, *36*, 122002. [[CrossRef](#)]
176. Li, C.; Fan, B.; Li, W.; Wen, L.; Liu, Y.; Wang, T.; Sheng, K.; Yin, Y. Bandgap engineering of monolayer MoS<sub>2</sub> under strain: A DFT study. *J. Korean Phys. Soc.* **2015**, *66*, 1789–1793. [[CrossRef](#)]
177. Li, T.; Galli, G. Electronic properties of MoS<sub>2</sub> nanoparticles. *J. Phys. Chem. C* **2007**, *111*, 16192–16196. [[CrossRef](#)]
178. Bollinger, M.V.; Jacobsen, K.W.; Nørskov, J.K. Atomic and electronic structure of MoS<sub>2</sub> nanoparticles. *Phys. Rev. B Condens. Matter Mater. Phys.* **2003**, *67*, 085410. [[CrossRef](#)]
179. Javaid, M.; Drumm, D.W.; Russo, S.P.; Greentree, A.D. A study of size-dependent properties of MoS<sub>2</sub> monolayer nanoflakes using density-functional theory. *Sci. Rep.* **2017**, *7*, 9775. [[CrossRef](#)]
180. Liu, X.; Cao, D.; Yang, T.; Li, H.; Ge, H.; Ramos, M.; Peng, Q.; Dearden, A.K.; Cao, Z.; Yang, Y.; et al. Insight into the structure and energy of Mo<sub>27</sub>S<sub>x</sub>O<sub>y</sub> clusters. *RSC Adv.* **2017**, *7*, 9513–9520. [[CrossRef](#)]

181. Li, N.; Lee, G.; Jeong, Y.H.; Kim, K.S. Tailoring Electronic and Magnetic Properties of MoS<sub>2</sub> Nanotubes. *J. Phys. Chem. C* **2015**, *119*, 6405–6413. [[CrossRef](#)]
182. Wang, R.; Sun, H.; Ma, B.; Hu, J.; Pan, J. Edge passivation induced single-edge ferromagnetism of zigzag MoS<sub>2</sub> nanoribbons. *Phys. Lett. A* **2017**, *381*, 301–306. [[CrossRef](#)]
183. Li, Y.; Zhou, Z.; Zhang, S.; Chen, Z. MoS<sub>2</sub> Nanoribbons: High Stability and Unusual Electronic and Magnetic Properties. *J. Am. Chem. Soc.* **2008**, *130*, 16739–16744. [[CrossRef](#)] [[PubMed](#)]
184. Raybaud, P.; Hafner, J.; Kresse, G.; Kasztelan, S.; Toulhoat, H. Ab Initio Study of the H<sub>2</sub>–H<sub>2</sub>S/MoS<sub>2</sub> Gas–Solid Interface: The Nature of the Catalytically Active Sites. *J. Catal.* **2000**, *189*, 129–146. [[CrossRef](#)]
185. Li, S.; Liu, Y.; Feng, Z.; Chen, X.; Yang, C. Insights into the reaction pathway of thiophene hydrodesulfurization over corner site of MoS<sub>2</sub> catalyst: A density functional theory study. *Mol. Catal.* **2019**, *463*, 45–63. [[CrossRef](#)]
186. Bonde, J.; Moses, P.G.; Jaramillo, T.F.; Nørskov, J.K.; Chorkendorff, I. Hydrogen evolution on nano-particulate transition metal sulfides. *Faraday Discuss.* **2009**, *140*, 219–231. [[CrossRef](#)]
187. Wang, H.; Tsai, C.; Kong, D.; Chan, K.; Abild-Pedersen, F.; Nørskov, J.K.; Cui, Y. Transition-metal doped edge sites in vertically aligned MoS<sub>2</sub> catalysts for enhanced hydrogen evolution. *Nano Res.* **2015**, *8*, 566–575. [[CrossRef](#)]
188. Jin, Q.; Chen, B.; Ren, Z.; Liang, X.; Liu, N.; Mei, D. A theoretical study on reaction mechanisms and kinetics of thiophene hydrodesulfurization over MoS<sub>2</sub> catalysts. *Catal. Today* **2018**, *312*, 158–167. [[CrossRef](#)]
189. Silva, A.M.; Borges, I. How to find an optimum cluster size through topological site properties: MoS<sub>x</sub> model clusters. *J. Comput. Chem.* **2011**, *32*, 2186–2194. [[CrossRef](#)]
190. Yang, T.; Feng, J.; Liu, X.; Wang, Y.; Ge, H.; Cao, D.; Li, H.; Peng, Q.; Ramos, M.; Wen, X.-D.; et al. A combined computational and experimental study of the adsorption of sulfur containing molecules on molybdenum disulfide nanoparticles. *J. Mater. Res.* **2018**, *33*, 3589–3603. [[CrossRef](#)]
191. Gronborg, S.S.; Saric, M.; Moses, P.G.; Rossmesl, J.; Lauritsen, J.V. Atomic scale analysis of sterical effects in the adsorption of 4,6-dimethyldibenzothiophene on a CoMoS hydrotreating catalyst. *J. Catal.* **2016**, *344*, 121–128. [[CrossRef](#)]
192. Deng, J.; Li, H.; Xiao, J.; Tu, Y.; Deng, D.; Yang, H.; Tian, H.; Li, J.; Ren, P.; Bao, X. Triggering the electrocatalytic hydrogen evolution activity of the inert two-dimensional MoS<sub>2</sub> surface via single-atom metal doping. *Energy Environ. Sci.* **2015**, *8*, 1594. [[CrossRef](#)]
193. Sharma, A.; Srivastava, A.; Husain, M.; Khan, M.S. Computational investigations of Cu-embedded MoS<sub>2</sub> sheet for CO oxidation catalysis. *J. Mater. Sci.* **2018**, *53*, 9578–9588. [[CrossRef](#)]
194. Zhang, Y.-H.; Chen, J.-L.; Yue, L.-J.; Zhang, H.-L.; Li, F. Tuning CO sensing properties and magnetism of MoS<sub>2</sub> monolayer through anchoring transition metal dopants. *Comput. Theor. Chem.* **2017**, *1104*, 12–17. [[CrossRef](#)]
195. Ding, K.; Lin, Y.; Huang, M. The enhancement of NO detection by doping strategies on monolayer MoS<sub>2</sub>. *Vacuum* **2016**, *130*, 146–153. [[CrossRef](#)]
196. Pan, H. *Progress on the Theoretical Study of Two-Dimensional MoS<sub>2</sub> Monolayer and Nanoribbon*; Springer: Cham, Switzerland, 2014; pp. 1–35.
197. Aray, Y.; Rodríguez, J.; Vidal, A.B.; Coll, S. Nature of the NiMoS catalyst edge sites: An atom in molecules theory and electrostatic potential studies. *J. Mol. Catal. A Chem.* **2007**, *271*, 105–116. [[CrossRef](#)]
198. Xu, C.; Shi, Q. *Structure and Modeling of Complex Petroleum Mixtures*; Springer: Cham, Switzerland, 2015.
199. Prabowo, W.A.E.; Kemal Agusta, M.; Lubis, A.H.; Dipojono, H.K. Density Functional Theory Study of the Adsorption of Thiophene on NiMoS Surface. In Proceedings of the International MultiConference of Engineers and Computer Scientists, Hong Kong, China, 13–15 March 2013; Ao, S.I., Castillo, O., Douglas, C., Feng, D.D., Korsunsky, A.M., Eds.; Newswood Limited: Hong Kong, China, 2013; pp. 13–15.
200. Ruinart de Brimont, M.; Dupont, C.; Daudin, A.; Geantet, C.; Raybaud, P. Deoxygenation mechanisms on Ni-promoted MoS<sub>2</sub> bulk catalysts: A combined experimental and theoretical study. *J. Catal.* **2012**, *286*, 153–164. [[CrossRef](#)]
201. Moses, P.G.; Hinnemann, B.; Topsøe, H.; Nørskov, J.K. The effect of Co-promotion on MoS<sub>2</sub> catalysts for hydrodesulfurization of thiophene: A density functional study. *J. Catal.* **2009**, *268*, 201–208. [[CrossRef](#)]
202. Ding, S.; Jiang, S.; Zhou, Y.; Wei, Q.; Zhou, W. Catalytic characteristics of active corner sites in CoMoS nanostructure hydrodesulfurization—A mechanism study based on DFT calculations. *J. Catal.* **2017**, *345*, 24–38. [[CrossRef](#)]

203. Šarić, M.; Rossmeisl, J.; Moses, P.G. Modeling the active sites of Co-promoted MoS<sub>2</sub> particles by DFT. *Phys. Chem. Chem. Phys.* **2017**, *19*, 2017–2024. [[CrossRef](#)] [[PubMed](#)]
204. Šarić, M.; Rossmeisl, J.; Moses, P.G. Modeling the adsorption of sulfur containing molecules and their hydrodesulfurization intermediates on the Co-promoted MoS<sub>2</sub> catalyst by DFT. *J. Catal.* **2018**, *358*, 131–140. [[CrossRef](#)]
205. Laurent, E.; Delmon, B. Study of the hydrodeoxygenation of carbonyl, carboxylic and guaiacyl groups over sulfided CoMo/γ-Al<sub>2</sub>O<sub>3</sub> and NiMo/γ-Al<sub>2</sub>O<sub>3</sub> catalyst: II. Influence of water, ammonia and hydrogen sulfide. *Appl. Catal. A Gen.* **1994**, *109*, 97–115. [[CrossRef](#)]
206. He, Z.; Wang, X. Hydrodeoxygenation of model compounds and catalytic systems for pyrolysis bio-oils upgrading. *Catal. Sustain. Energy* **2012**, *1*, 28–52. [[CrossRef](#)]
207. Oh, S.; Choi, H.S.; Choi, I.-G.; Choi, J.W. Evaluation of hydrodeoxygenation reactivity of pyrolysis bio-oil with various Ni-based catalysts for improvement of fuel properties. *RSC Adv.* **2017**, *7*, 15116–15126. [[CrossRef](#)]
208. Hensley, A.J.R.; Wang, Y.; Mei, D.; McEwen, J.-S. Mechanistic Effects of Water on the Fe-Catalyzed Hydrodeoxygenation of Phenol. The Role of Brønsted Acid Sites. *ACS Catal.* **2018**, *8*, 2200–2208. [[CrossRef](#)]
209. Badawi, M.; Paul, J.F.; Cristol, S.; Payen, E.; Romero, Y.; Richard, F.; Brunet, S.; Lambert, D.; Portier, X.; Popov, A.; et al. Effect of water on the stability of Mo and CoMo hydrodeoxygenation catalysts: A combined experimental and DFT study. *J. Catal.* **2011**, *282*, 155–164. [[CrossRef](#)]
210. Sun, M.; Nelson, A.E.; Adjaye, J. On the incorporation of nickel and cobalt into MoS<sub>2</sub>-edge structures. *J. Catal.* **2004**, *226*, 32–40. [[CrossRef](#)]
211. Krebs, E.; Silvi, B.; Raybaud, P. Mixed sites and promoter segregation: A DFT study of the manifestation of Le Chatelier's principle for the Co(Ni)MoS active phase in reaction conditions. *Catal. Today* **2008**, *130*, 160–169. [[CrossRef](#)]
212. Krebs, E.; Daudin, A.; Raybaud, P. A DFT Study of CoMoS and NiMoS Catalysts: From Nano-Crystallite Morphology to Selective Hydrodesulfurization Catalysts and Adsorbents: From Molecular Insight to Industrial Optimization Catalyseurs et adsorbants: De la compréhension moléculaire à l'optimisation industrielle. *Oil Gas Sci. Technol. IFP* **2009**, *64*, 707–718.
213. Badawi, M.; Paul, J.-F.; Payen, E.; Romero, Y.; Richard, F.; Brunet, S.; Popov, A.; Kondratieva, E.; Gilson, J.-P.; Mariey, L.; et al. Hydrodeoxygenation of Phenolic Compounds by Sulfided (Co)Mo/Al<sub>2</sub>O<sub>3</sub> Catalysts, a Combined Experimental and Theoretical Study. *Oil Gas Sci. Technol.* **2013**, *68*, 829–840. [[CrossRef](#)]
214. Czekaj, I.; Wambach, J.; Kröcher, O. Modelling catalyst surfaces using DFT cluster calculations. *Int. J. Mol. Sci.* **2009**, *10*, 4310–4329. [[CrossRef](#)] [[PubMed](#)]
215. Hinnemann, B.; Nørskov, J.K.; Topsøe, H. A density functional study of the chemical differences between type I and type II MoS<sub>2</sub>-based structures in hydrotreating catalysts. *J. Phys. Chem. B* **2005**, *109*, 2245–2253. [[CrossRef](#)] [[PubMed](#)]
216. Topsøe, H.; Hinnemann, B.; Nørskov, J.K.; Lauritsen, J.V.; Besenbacher, F.; Hansen, P.L.; Hytoft, G.; Egeberg, R.G.; Knudsen, K.G. The role of reaction pathways and support interactions in the development of high activity hydrotreating catalysts. *Catal. Today* **2005**, *107–108*, 12–22. [[CrossRef](#)]
217. Costa, D.; Arrouvel, C.; Breyse, M.; Toulhoat, H.; Raybaud, P. Edge wetting effects of γ-Al<sub>2</sub>O<sub>3</sub> and anatase-TiO<sub>2</sub> supports by MoS<sub>2</sub> and CoMoS active phases: A DFT study. *J. Catal.* **2007**, *246*, 325–343. [[CrossRef](#)]

